The isotopic study on solid precipitation from a convective cloud: Observation and modeling

（対流雲がもたらす降雪粒子の安定同位体組成に関する研究：観測と数値計算）

Atsuko Sugimoto

杉本敦子

主論文

The isotopic study on solid precipitation from a convective cloud: Observation and modeling

（対流雲がもたらす降雪粒子の安定同位体組成に関する研究：観測と数値計算）

Atsuko Sugimoto

杉本敦子

Contents

Abstract

The isotopic composition of solid precipitation depends on the following processes: evaporation from the sea surface, condensation and sublimation of cloud particles, fromation of these particles into precipitation and dynamic process of the cloud itself. To clarify the behavior of water isotopes in each process from the observation of solid precipitation at the surface, observations at two stations along a cloud trajectory and the numerical modeling of a precipitation process were made on the isotopic composition of solid precipitation generating from a convective cloud.

The observations were made at two stations 8 km apart along a cloud trajectory at Ishikari plain in 1985 and 1986, and at two stations 30 km apart in Hokuriku in 1983.

The δD and $\delta^{18}O$ values of snow particles from a separate cloud or a radar echo which consists of several cells were linearly related. The values of deuterium excess of observed δD-$\delta^{18}O$ relations were much greater than 10 and differed with each case, while the slope was 8.5 - 9.6 in 7 of 9 cases.

Several conclusions about the evaporation process can be drawn from these observations. First, a cloud which produced solid precipitation observed at the two sites consists of air parcels containing initial water vapor with the same isotopic composition. Second, the isotopic composition of initial water vapor which makes a cloud differs from case to case. Finally, the observed large deuterium excess is caused by kinetic evaporation from the sea surface, and is too large to be explained by Merlivat and Jouzel's (1979) model.

Linearity between δD and $\delta^{18}O$ of precipitation made it

possible to clarify fractionation during condensation and sublimation of cloud particles. The observed slopes of δD-$\delta^{18}O$ relations indicate that the value of $(\alpha_D-1)/(\alpha_{18O}-1)$ during condensation is close to that determined by Merlivat and Nief (1967) and Majoube (1971) under isotopic equilibrium, while that during sublimation is 8 % larger than that determined by Merlivat and Nief (1967) and Majoube (1970) under isotopic equilibrium, due to kinetic effects. The model by Jouzel and Merlivat (1984) explains the observed enlargement of the value of $(\alpha_D-1)/(\alpha_{18O}-1)$.

The constancy of the isotopic composition of initial water vapor in a cloud also made it possible to discuss the precipitation process which includes condensation and sublimation of cloud particles, formation of these particles into precipitation and the dynamic process of the cloud itself, from the difference in the $\delta^{18}O$ of solid precipitation from a convective cloud observed between the two stations 8 km apart along the cloud trajectory. The $\delta^{18}O$ values of snow from a convective cloud decrease with time during its lifetime; the rate of decrease observed in 7 cases of convective radar echoes was 0.2 to 3.1‰ during 15 min of movement of radar echoes between two stations, and was large during and after its maximum precipitation intensity. The rate of decrease was high in cells in which precipitation was intense in the windward area, and a very small decrease (0.2‰) was observed in an underdeveloped cell.

A one-dimensional time-dependent model is used to calculate the isotopic variation of solid precipitation during the lifetime

of a convective cloud cell. The calculated results explain the observed results well. In addition, calculated results show that the rate of decrease of $\delta^{18}O$ is large in cells with high precipitation efficiency, and in cells with large terminal velocity of precipitating particles. The model results also indicate that the more precipitation has fallen from a cell, the smaller $\delta^{18}O$ of solid precipitation from the cell.

1 Introduction

The isotopic composition of precipitation is expressed by δ values as:

$$\delta^{18}O\ (\delta D) = (R_{sample} - R_{SMOW})/R_{SMOW} \times 1000\ (‰)$$

where R_{sample} and R_{SMOW} are the isotopic ratios ($H_2{}^{18}O/H_2{}^{16}O$ or $HDO/H_2{}^{16}O$) of a sample and SMOW (Standard Mean Ocean Water) respectively.

The abundance of water isotopes changes during the phase change of water molecules or isotopic exchange between different phases. Each isotope reaction obeys the Law of Mass Action and can be described by an isotope fractionation factor (α). Fractionation factors between water vapor and liquid (α_{l-v}), between water vapor and ice (α_{i-v}) and between liquid and ice (α_{i-l}) are defined as follows;

$$\alpha_{l-v} = R_l/R_v$$

$$\alpha_{i-v} = R_i/R_v$$

$$\alpha_{i-l} = R_i/R_l$$

where R_v, R_l and R_i are the isotopic ratios in water vapor, liquid and ice. Under isotopic equilibrium, the values of α are slightly larger than 1 and increase with decreasing temperature.

Craig (1961) showed that the annual mean δD and $\delta^{18}O$ values of worldwide precipitation show a linear relationship, $\delta D = 8\delta^{18}O + 10$. This line is called the "meteoric water line" (MWL). On the other hand, the δD-$\delta^{18}O$ relationship of individual precipitation often differs from MWL. In order to relate the composition of any sample to MWL, Dansgaard (1964) defined the "d-index" as $d = \delta D - 8\delta^{18}O$. Such a value is also called "deuterium excess", "d-value" or "d-parameter". The

term "deuterium excess" is used here.

Dansgaard (1964) pointed out the relation between annual mean $\delta^{18}O$ and surface air temperature, namely low $\delta^{18}O$ with low air temprerature (the temperature effect). This relation is also called the "latitude effect", since annual mean air temperature is low at high latitudes. The annual mean $\delta^{18}O$ has also been related to distance from the coast. The decrease of annual mean $\delta^{18}O$ with distance from the coast was shown in the Amazon basin by Salati et al. (1979) and on the European continent by Rozanski et al. (1982). These relations are the so-called "continental effect" or "inland effect". They explained these effects as instances of depleted water vapor re-evaporated from the surface.

Many studies on the seasonal variation of $\delta^{18}O$ or δD at a given station have been made on the basis of the monthly mean values. The relation, that is low values of monthly mean $\delta^{18}O$ on the month with much precipitation, was shown for many stations by Dansgaard (1964). This relation is called the "amount effect", and has also been reported in Japan, at Tokyo by Dansgaard (1964), at Nasudake by Kusakabe et al. (1976) and at Nagoya by Waseda and Nakai (1983). Dansgaard (1964) pointed out the amount effect was caused by depth of convection and evaporation and by isotope exchange between raindrops and environmental water vapor in and below a cloud. Yapp (1982) has shown that the correlation between the δD and precipitation intensity can exist under many assumptions such as constant isotopic composition of initial water vapor and constant initial condensation temperature. The "amount effect" is the result of

averaging over a longer time scale.

In the polar regions, the "temperature effect" on the basis of monthly mean values has been reported (Picciotto and De Maere, 1960; Epstein et al, 1963; Aldaz and Deutsch, 1967), and the $\delta^{18}O$ in Antarctic precipitation was also related to the distance from the open sea (Kato, 1978).

The annual mean or monthly mean values integrate of various types of precipitation. The isotopic composition of an individual storm was studied in relation with its trajectory. Lawrence et al. (1982) pointed out that the δD at New York was low because of the high altitude of the frontal surface when low pressure took a seaward path. Rindsberger et al. (1983) discussed the difference in modification of air mass with the trajectory of a storm in Mediterranean Sea area.

The negative correlation between the $\delta^{18}O$ of an individual precipitation event and altitude at sampling site (altitude effect) has been observed (Niewodniczanski et al., 1981; Waseda and Nakai, 1983). Higuchi (1982) discussed the "inland effect" of $\delta^{18}O$ in drifting snow in Antarctica from horizontal and vertical wind velocities.

The sampling time of an individual storm is too long to study the behavior of isotopes in each process, because a storm consists of several cloud systems which include many clouds. The isotopic composition of precipitation from a given cloud depends on the following processes:

(i) The δD and $\delta^{18}O$ of water vapor constituting a cloud depend on the evaporation process from the sea surface (or the earth's surface, plants, etc.), and on transportation and mixing processes.

(ii) Formation process of cloud particles in an air parcel; condensation of water vapor to cloud droplets and sublimation to ice crystals.

(iii) Formation process of precipitating particles in a cloud; growth of particles by condensation, sublimation, coalescence, accretion and aggregation in a cloud.

(iv) Dynamic process of a cloud.

(v) Evaporation and melting of precipitating particles and isotope exchange processes between precipitating particles and the environment in and below a cloud.

In the above processes, isotope fractionation occurs during evaporation, transportation of water vapor, condensation, sublimation and isotope exchange between precipitating particles and environmental water vapor.

The behavior of water isotopes during each process described above has been studied, chifely by means of theoretical and experimental approach.

Dansgaard (1964) pointed out that deuterium excess is caused by kinetic effect during evaporation (including upward transportation) of water vapor from the sea surface. Craig and Gordon (1965) proposed a theory for kinetic effect during evaporation, and discussed fractionation during upward transportation of water vapor by turbulence. However, their theory includes many unknown values such as condensation rates of isotopes. Merlivat and Jouzel (1979) modeled such a kinetic evaporation by means of parameterization, using Brutsaert's theory (1975a and b) and they calculated deuterium excess as a function of relative humidity above the sea. Their theoretical

study is the model for the evaporation process from the sea surface.

Fractionation factors during condensation and sublimation under isotopic equilibrium have been determined by experiments (Merlivat and Nief, 1967; Majoube, 1970, 1971). Model calculations of the isotopic composition of liquid and solid condensates in an air parcel were made by Dansgaard (1964), based on the Rayleigh condensation model in which condensates are removed immediately from the air parcel, and on the two-phase model in which condensates remain in the air parcel. In these models, isotope equilibrium is assumed. Non-equilibrium formation of snow particles has been modeled by Jouzel and Merlivat (1984). They have shown that kinetic effect during sublimation is caused by the difference in molecular diffusivity among $H_2{}^{16}O$, HDO and $H_2{}^{18}O$, accordingly, the slope of δD-$\delta^{18}O$ relation of snow slightly increases in a supersuturation with water vapor. These models express the formation process of cloud particles in an air parcel.

The isotopic composition of precipitation depends on many complicated factors. Therefore, it is difficult to clarify the behavior of water isotopes in each process in actual precipitation, based on the mean values. Nevertheless these models described above have been directly applied to data on a global scale or annual and monthly mean values. However, in order to understand the behavior of water isotopes in the actual cloud, it is necessary to study in detail a single instance of rainfall or snowfall.

The isotopic composition of precipitation offers a great deal of information on the water cycle, including water vapor sources

in the study of a storm. On the other hand, in an ice core study, the isotopic composition of precipitation has been used to estimate the paleoclimate. However, the $\delta^{18}O$-temperature relation is an empirical relation. Recently Jouzel et al. (1987) showed that the isotopic composition of precipitation can be calculated in a general circulation model (GCM). It is necessary to understand the present and past $\delta^{18}O$-temperature relation and δD-$\delta^{18}O$ relation and distribution on a global scale using GCMs in order to reconstruct the paleoclimate from the isotopic composition in ice core. Basic knowledge on the behavior of water isotopes is necessary for the calculation of the isotopic composition of atmospheric water and that in a convective cloud, in particular for isotopic parameterization of sub-grid scale cumulus convection in a GCM.

Up to now, short-term variation of $\delta^{18}O$ or δD values of precipitation has been discussed in connection with the evaporation and isotope exchange processes between raindrops and environment (Friedman et al., 1962; Woodcock and Friedman, 1963; Miyake et al., 1968), and in connection with the structure of a front (Miyake et al. 1968; Gedzelman and Lawrence 1982). Gedzelman and Lawrence (1982) also demonstrated non-linearity between δD and $\delta^{18}O$ of precipitation from a warm front. Non-linearity between δD and $\delta^{18}O$ of precipitation from a single storm has also been studied on large hailstones with regard to evaporation of liquid during freezing on the surface of hailstones by Federer et al. (1982b) and Jouzel et al. (1985). Evaporation disturbs the original δD-$\delta^{18}O$ relation of cloud particles. Their data, therefore, were not adequate to reveal

the behavior of stable isotopes in an individual process. It is necessary to observe the δD and $\delta^{18}O$ of solid precipitation from an individual cloud, since in the case of falling solid precipitation, the δD-$\delta^{18}O$ relation is not affected by evaporation.

Many "steady-state" cloud models which express the formation process of precipitating particles have been proposed to calculate the isotopic composition of hailstones (Macklin et al., 1970; Jouzel et al., 1975; Federer et al., 1982a). In all these models, except the last, the dynamic process cannot be expressed, because only the vertical distribution of $\delta^{18}O$ (or δD) of cloud droplets and water vapor can be calculated on the basis of Rayleigh or the two-phase model.

On the other hand, Miyake et al. (1968) and Fujiyoshi et al. (1986) showed that the $\delta^{18}O$ of snow particles varied by accretion of cloud droplets from the observations of short-term variation of $\delta^{18}O$ at a fixed observation station. Their studies indicate the importance of the precipitation process.

However, a cloud is not "steady-state," particularly not a convective cloud. The isotopic composition of precipitation from a convective cloud might vary with time; to find out, it is necessary to collect precipitation from a cloud at more than two sites along the cloud trajectory. Then, a time-dependent cloud model is necessary to express the precipitation porcess in a convective cloud, which should include the formation processes of cloud particles and precipitating particles and also the dynamic process of the cloud.

For these purpose, in the present study, the δD and $\delta^{18}O$ values are investigated on solid precipitation during the winter

monsoon along the Sea of Japan.

When a cold and dry air mass breaks out from the Siberian continent to the Sea of Japan in winter, it is modified by heat and water vapor supplied from the relatively warm sea surface. Many convective clouds develop over the Sea of Japan. Such convective clouds produce precipitation in the coastal region along the Sea of Japan, but become weak inland due to the decrease of heat and water vapor supply. Therefore, it is possible to collect snow samples at different stages of the same cloud when two observation stations can be set along the trajectory of the cloud.

In the snowfall investigated here, some processes can be simplified. First, the origin of water vapor is almost entirely from the Sea of Japan. Second, there is practically no exchange of isotopes between precipitating snow particles and environment because of low diffusivity of water molecules in ice (10^{-15} m^2/sec at -10 °C) as determined by Itagaki (1967). Third, a cloud responsible for the precipitation is relatively simple and small, compared with those for fronts and typhoons.

Many investigations have been made on the isotopic compositions of the snowfall during the winter monsoon along the Sea of Japan. The deuterium excess of river water in the region along the Sea of Japan is higher than that along the Pacific Ocean (Matsubaya and Sakai, 1976). Matsubaya and Etchu (1987) showed that the deuterium excess of spring water in Omono drainage depends on the ratio of winter precipitation to annual precipitation. In the region along the Sea of Japan, monthly mean values of dueterium excess are higher (about 30) in winter

than in the other seasons (about 10), due to fast evaporation from the Sea of Japan (Satake et al., 1982).

Tsunogai et al. (1975) sampled the snow which fell for two to 10 hours all together, and showed that the $\delta^{18}O$ was small during a passage of a front and increased after its passage. Geographical $\delta^{18}O$ distribution around the mountain was observed by Watanabe et al. (1986). They showed that the rate of decrease of $\delta^{18}O$ with the distance from the coast differs with the slope.

On the other hand, short-term variations of $\delta^{18}O$ were also observed. Increase of $\delta^{18}O$ during the passage of a cloud was shown by Miyake et al. (1968). They explained that the $\delta^{18}O$ increases because the large particles growing in higher parts of the cloud arrived earlier at the surface due to large falling velocity. Fujiyoshi et al. (1986) observed the relation between the $\delta^{18}O$ and crystal shape and degree of accretion of cloud droplets, and they pointed out that the effect of accretion of cloud droplets on the $\delta^{18}O$ differs with the height of accretion. The $\delta^{18}O$ variations observed at only one site as studied by Miyake et al. (1968) and Fujiyoshi et al. (1986) reflect the heterogenious horizontal structure of the cloud.

Many studies on clouds themselves have also been made. In this region a band-shaped cloud in which convective clouds line up is sometimes observed. Up to now, such band-shaped clouds have been well observed, and their decay after landfall has also been observed. Magono (1965) showed that the tops of the band-shaped clouds change from scalloped to smoothed as they moving inland, due to decay of convection, according to movie camera observations along the Ishikari plain. Downdraft under the

cloud which was precipitating graupels was also observed at the Ishikari plain by Higuchi (1963).

It is well-known that a convective cloud consists of several regions which have different stages. Such a region is denoted by the "cell" below. Generally, the life of a cell is divided into three stages; developing, mature and decaying, and its lifetime is about 1 hour. The cells in the convective cloud observed here were considered to be in the various stages at the time of their landfall.

Separate sampling of snow particles from individual cells is the best way to reveal the behavior of isotopes in each process. However, such sampling is not easy, since identification of snow particles from individual cells is difficult. Accordingly, in the case of band-shaped clouds, when a convective radar echo was identified from radar observation, snow particles from each echo were sampled at both stations. In the case of isolated clouds, that from each cloud were sampled. Then, the $\delta^{18}O$ values from each echo or each cloud were compared between the two stations.

The purpose of this study is to know the behavior of water isotopes in each process in the actual convective cloud: to know the isotopic composition of water vapor constituting a cloud, to clarify the fractionation during condensation and sublimation of cloud particles in an air parcel, to clarify the effect of precipitation process on the isotopic composition of precipitation, from the isotopic composition of solid precipitation observed at the surface, and then to make a time-dependent isotopic cloud model.

For this purpose, the δD and $\delta^{18}O$ values in solid

precipitation from an individual convective cloud are observed at two stations along the trajectory of the cloud.

2 Methods of observations and isotopic analyses

Sampling was carried out in two regions, Ishikari plain, Hokkaido and Hokuriku, shown in Fig. 2-1. The two stations were set along the direction of the prevailing wind, NW; the distance between them was 8 km in Ishikari plain and 30 km in Hokuriku. As seen in Fig. 2-1, the windward station situated about 4 km from the coast in Ishikari plain, and 13 km in Hokuriku.

The geographical conditions are different between the two regions; there is no mountain between the two stations in Ishikari plain, while there is a high mountain ridge (about 1500m a.s.l.) in Hokuriku, where convective clouds are modified by orographic lifting. Then, the results observed in Ishikari plain are chiefly mensioned here, to focus the isotopic comosition of solid precipitation from a convective cloud.

Various types of convective cloud besides band-shaped cloud were observed in both regions. Comparing between Ishikari plain and Hokuriku, the cloud scale is larger in Hokuriku.

Falling snow particles were collected on PVC trays, over periods ranging from 5 minutes to several tens of minutes. Each snow sample was kept in a vial to avoid evaporation until it was analyzed.

Observation of precipitation intensity and type of snow particles were made at the same time. Radar observations were carried out at the leeward station in Ishikari plain by a group from the Institute of Low Temperature Science, Hokkaido University. Accordingly, the observed clouds could be followed during traveling from the coast to the leeward station by radar observation. The observed variation is divided into each cloud

or radar echo and the isotopic comosition of solid precipitation generating from each cloud or radar echo is considered below.

Oxygen isotopic analysis was carried out with a MAT250 mass spectrometer on CO_2 equilibrated with sample water, and hydrogen isotopic analysis with HITACHI RMD mass spectrometer on H_2 reduced from sample water using heated uranium. Isotopic composition was expressed in terms of δD and $\delta^{18}O$ (‰) relative to V-SMOW. The analytical error was less than 0.2‰ for $\delta^{18}O$ and 1 ‰ for δD.

3 Observed variations of $\delta^{18}O$ of solid precipitation

In this section, general aspects on the variations of the isotopic composition of falling snow observed in Hokuriku are described.

i) Hourly variations of the $\delta^{18}O$

Time variations of 6 hours running mean $\delta^{18}O$ of falling snow observed at two stations on Feb. 7 to 13, 1983 in Hokuriku are shown in Fig. 3-1. The $\delta^{18}O$ values show large fluctuation and also show the good correlation with surface air temperature, namely the smaller the $\delta^{18}O$ in the colder condition. Comparing the $\delta^{18}O$ values between the two stations, they are similar in variations and those at leeward station, Shirakawa, are smaller than those at windward station, Tsurugi. The difference between the two stations is 1 to 3 ‰ with the time lag about 30 min to 1 hour throughout the observation period. The range of fluctuation observed here is the same as that observed by Tsunogai et al. (1975).

ii) Time variation of the $\delta^{18}O$ during the passage of a cloud

Short-term variations of $\delta^{18}O$ have various patterns. Fig. 3-2 shows the case of Feb.7, 1983 at Tsurugi, when small graupels and rimed snowflakes were observed. In this case, the $\delta^{18}O$ decrease during the passage of a cloud. Miyake et al. (1968) reported the increase of $\delta^{18}O$ during the passage of a cloud. Each variation which corresponds to the passage of a cloud is caused by the variation of $\delta^{18}O$ during the lifetime of a convective cloud and the horizontal structure of the cloud due to wind shear.

4 Relationship between δD and $\delta^{18}O$ values of solid precipitation from a convective cloud

In this section, the evaporation process from the sea surface and the formation process in an air parcel are described from the δD-$\delta^{18}O$ relation of the solid precipitation from an individual cloud or a radar echo.

4.1 The observed δD-$\delta^{18}O$ relation

Among the many cases obtained from the observation, 9 cases (A to I) were chosen, in which range of $\delta^{18}O$ of snow particles produced in the cloud was large enough to discuss δD-$\delta^{18}O$ relation. These 9 cases tarbulated in Table 4-1 will be described.

The δD-$\delta^{18}O$ relations of snow collected at two stations for cases A to I are shown in Fig. 4-1. For each case, type of falling snow particles, height of echo top of precipitating cloud and surface air temperature at the time of collection are given in Table 4-1. Each case corresponds to a separate cloud or a radar echo. For each case, the cloud was confirmed to pass over both stations by radar observation and also by comparison of precipitation intensity except in cases D, E and F when the sampling was done at only one station.

As seen in Fig. 4-1, a linear relation exists between the δD and $\delta^{18}O$ values of falling snow particles produced in a separate cloud or a radar echo and collected at two stations, and the δD and $\delta^{18}O$ values at the windward station are higher than those at the leeward station. The isotopic difference between the two stations will be discussed in chapter 5.

The regression line for each case is also shown in Fig. 4-1.

Slopes of these lines are 8.5 - 9.6 in 7 of 9 cases, with a maximum of 15 and minimum of 7.4.

In case C, the slope is calculated to have a minimum of 7.4. However, it can be noted that data points are on the two almost parallel lines (broken lines, in Fig. 4-1 case C), one of which is almost identical with that for cases A and B with a slope of 9.6.

A comparison of the Ishikari plain results with those from Hokuriku shows that the slopes are not so different.

The type of snow particles is important when considering the formation process of particles. However, no difference is found in slope among the cases in which only graupels (cases A, B and C), graupels and non-rimed snowflakes (case D), only non-rimed snowflakes (case E), and graupels and rimed snowflakes (cases F to I) were observed.

Fig. 4-2 shows nine regression lines for each case and the meteoric water line (MWL). All lines are above the MWL. The lines for cases A to F, obtained in Ishikari plain, are above those for cases G to I, obtained in Hokuriku where the air is warmer and moister than in Ishikari plain. This can be explained by the difference in isotopic composition of the initial vapor from which falling snow particles are formed.

4.2 The isotopic composition of initial water vapor in a cloud

Generally, a snow particle grows after sublimation, accretion of cloud droplets and coalescence among crystals. Isotope fractionation takes place during sublimation and condensation of water vapor on a snow crystal and cloud droplet, and is negligible in coalescence and accretion as calculated by

Jouzel et al. (1985), when the surface temperature on a particle is lower than 0 °C.

In the case of graupel, the mass formed by accretion of cloud droplets is much larger than that formed by sublimation, so that it can be assumed that graupel is made of cloud droplets so far as isotopic composition is concerned. Therefore, the δD-$\delta^{18}O$ relation of graupels is discussed on the basis of the two phase model of cloud droplets by Merlivat and Jouzel (1979).

When the air parcel ascends and cloud droplets grow in it, the isotopic concentration ($HDO/H_2{}^{16}O$ or $H_2{}^{18}O/H_2{}^{16}O$) of water vapor in the parcel R_v is calculated from

$$\frac{dR_v}{R_v} = \frac{-Ld\alpha + (\alpha - 1)dV}{V + L} \qquad (4\text{-}1)$$

where L and V are mixing ratio of liquid water (cloud droplets) and water vapor in the air parcel, and α (α_D for HDO or α_{18O} for $H_2{}^{18}O$) is the fractionation factor between liquid and water vapor. The δ values of cloud droplets at each height δ_c (δD_c for HDO or $\delta^{18}O_c$ for $H_2{}^{18}O$) are obtained from

$$\delta_c = \left\{ \frac{R_v}{R_{SMOW}} - 1 \right\} \times 1000 \quad (‰) \qquad (4\text{-}2)$$

From Eqs. (4-1), (4-2) and thermodynamic equation, the δD_c and $\delta^{18}O_c$ at each height can be calculated step by step, if and L at each height and the isotopic composition of water vapor at cloud base ($\delta D_v{}^0$ and $\delta^{18}O_v{}^0$) are given.

The calculated δD_c and $\delta^{18}O_c$ are almost linearly related if $(\alpha_D-1)/(\alpha_{18O}-1)$ is nearly constant. Fig. 4-3 shows the δD_c-$\delta^{18}O_c$ relations calculated for various $\delta D_v{}^0$ and $\delta^{18}O_v{}^0$, assuming L = 0 in Eq. (4-1). The value of $(\alpha_D-1)/(\alpha_{18O}-1)$ controls the slope of the δD_c-$\delta^{18}O_c$ relation, as will be described in section

4.4. The deuterium excess (defined by $\delta D - 8\delta^{18}O$) in the δD_c-$\delta^{18}O_c$ relation depends on the isotopic composition of initial vapor (δD_v^0 and $\delta^{18}O_v^0$), as seen in Fig. 4-3. The slope and deuterium excess are almost independent of L.

Therefore, if the initial vapor in all air parcels in a cloud has the same values of δD_v^0 and $\delta^{18}O_v^0$, the δD_c-$\delta^{18}O_c$ relation of all cloud droplets in the cloud should be linear. Since a graupel is made of cloud droplets as mensioned above, the δD-$\delta^{18}O$ relation of graupels produced in such cloud should be the same linear one as that of cloud droplets. On the contrary, if some air parcels contain water vapor having different isotopic composition from other parcels in the cloud, the δD_c-$\delta^{18}O_c$ relation of cloud droplets should not be linear.

Snowflakes are formed by coalescence of snow crystals which grew by sublimation. The δD and $\delta^{18}O$ values of snow crystals can also be calculated in a similar way to those of cloud droplets. The difference in condition between snow crystals and cloud droplets is only that there is no homogenization of isotopes in ice because of low diffusivity of water molecules in ice. The calculated δD-$\delta^{18}O$ relation of snow crystals is linear, similar to that of cloud droplets.

Therefore, the observed linear δD-$\delta^{18}O$ relation indicates that observed snow particles at the two stations are made from water vapor having the same isotopic composition. As seen in Fig. 4-1, linear δD-$\delta^{18}O$ relations are observed, in all cases except for C and I. Therefore, in the case of relatively small convective clouds as described here, a cloud consists of air parcels which contain initial vapor having the same isotopic

composition.

In the case C, the regression line for the leeward station is different from that for the windwared station, as shown in Fig. 4-1. Accordingly, graupels observed at the leeward station (open circles) were possibly formed from initial vapor having the isotopic composition, different from that which formed graupels observed at the windward station (closed circles).

4.3 The isotopic composition of initial water vapor and fractionation during evaporation from the sea surface

For cases A to H, the slope s and intercept d of the observed relation $\delta D = s\delta^{18}O + d$ are shown in Table 4-2. The observed values of d vary from case to case, namely 30 - 71, except for case I, and they are much greater than 10. If the values of deuterium excess are defined by $(\delta D - 8\delta^{18}O)$, they are also much greater than 10, that is the deuterium excess of MWL.

Such high deuterium excess values and their variation depend on the isotopic composition of initial vapor, as seen in Fig. 4-3. According to Merlivat and Jouzel (1979), the isotopic composition of water vapor evaporated from sea the surface depends on the relative humidity of the lower atmosphere. Snow particles studied here are made from water vapor which evaporates in blowing cold and dry air masses from the Siberian Continent on the relatively warm sea surface. Accordingly, relative humidity at the time of evaporation is considered to be low. Therefore, the high deuterium excess values described above can be explained qualitatively by low relative humidity, as discussed by Merlivat and Jouzel (1979).

In Fig. 4-3, broken lines are the calculated $\delta D - \delta^{18}O$

relations on the basis of the isotopic compositions of initial vapor calculated by their model for different relative humidity. But, the deuterium excess of the line for relative humidity R.H.=0 % is smaller than that for the observed relation in case B which is shown by the solid line in Fig. 4-3. Therefore, the very high deuterium excess cannot be explained quantitatively by their model. This suggests that it might be explained by a model including more effective molecular diffusion during transportation of water vapor in the atmospheric boundary layer as discussed by Craig and Gordon (1965).

4.4 Fractionations during condensation and sublimation

As seen in Table 4-2, the observed slopes of δD-$\delta^{18}O$ relation are 8.5 - 9.6, except for case I. These values will be compared with the slope for cloud droplets s_{eql} (liquid) and that for snow crystals s_{eqs} (solid) calculated on the assumption of isotopic equilibrium.

To calculate s_{eql} and s_{eqs}, the isotopic composition of initial water vapor is estimated, extending beyond the δD and $\delta^{18}O$ calculated by Merlivat and Jouzel's (1979) model for R. H. = 0 %, as shown in Fig. 4-3. After the isotopic composition of initial vapor (δD_v^0 and $\delta^{18}O_v^0$) for each case was estimated by means of the method shown in Fig. 4-3, the δD and $\delta^{18}O$ values of cloud droplets and snow crystals are calculated from Eqs. (4-1) and (4-2), using fractionation factors determined by Merlivat and Nief (1967), Majoube (1970) and Majoube (1971) under isotopic equilibrium. At first, initial temperature at the lifting condensation level was assumed for each case. Then, the slope of the δD-$\delta^{18}O$ relation of cloud droplets s_{eql} and that of snow

crystals s_{eqs} are calculated. The values of s, s_{eql}, s_{eqs}, δD_v^0, $\delta^{18}O_v^0$ and initial temperature are shown in Table 4-3.

The values of δD_v^0 and $\delta^{18}O_v^0$ affect the calculated slopes s_{eql} and s_{eqs}, as estimated by the following equation by Merlivat and Jouzel (1979) and Jouzel and Souchez (1982),

$$s_{eq} = \frac{1000 + \delta D_v^0}{1000 + \delta^{18}O_v^0} \frac{\alpha_D - 1}{\alpha_{180} - 1} \qquad (4\text{-}3)$$

where, s_{eq}, α_D and α_{180} are the mean values for a continuous condensation (or sublimation) process in a cloud. However, errors of s_{eql} and s_{eqs} due to estimation of δD_v^0 and $\delta^{18}O_v^0$ values are small, because the errors in them are much smaller than 1000.

As seen in Table 4-3, in almost all cases, the observed slopes roughly agree with the calculated slope s_{eql} for isotopic equilibrium condensation, or slightly larger than s_{eql}. In the cases of A, B and C in which graupels were observed, agreement between s and s_{eql} suggest that the value of $(\alpha_D-1)/(\alpha_{180}-1)$ is close to that under isotopic equilibrium during condensation of water vapor on cloud droplets.

In cases D and E in which non-rimed snowflakes were mainly observed, the observed values of s are not in agreement with s_{eqs}, namely, s is about 8 % greater than s_{eqs}. Such results can be explained by the theory of Jouzel and Merlivat (1984). They said that the values of $(\alpha_D-1)/(\alpha_{180}-1)$ depend on supersaturation of water vapor during growth of snow crystals by sublimation. According to their theory, the slope for snowflakes consisting of snow crystals is estimated to be about 8 % greater than the calculated value under equilibrium, when supersaturation of water vapor over ice is 5 % at -10°C, which is

suitable for growth of snow crystals.

In cases F, G and H in which both graupels and snowflakes were observed, it is considered that the slope for snowflakes became the same as that for graupels due to non-equilibrium sublimation as described above.

When a cloud droplet grows, as well as snow crystal, the air around it should be supersaturated with water vapor. Accordingly, the observed slope for graupels cannot agree with the calculated slope for equilibrium condensation s_{eql}, because of non-equilibrium condensation. However, observed slopes for grapels agree with calculated slope for equilibrium condensation. For this fact one possible explanation is that, as compared with supersaturation over ice, that over water is small in a cloud.

4.5 Conclusion

Follows are concluded on the isotopic composition of initial water vapor, on the fractionation during evaporation from the sea surface and on the fractionation during formation process of cloud particles, from the observed δD-$\delta^{18}O$ relations.

For the isotopic composition of initial water vapor and the evaporation process:

(1) The δD and $\delta^{18}O$ values of falling snow particles produced in a separate cloud or a radar echo have a linear relationship. It can be concluded from such linearity that a cloud which produced falling snow particles observed at two stations consistes of air parcels containing initial water vapor with the same isotopic composition.

(2) The observed values of deuterium excess were much greater than 10, and they differed from case to case. The variations

of deuterium excess indicate that the isotopic composition of initial water vapor which made a cloud differs from case to case.

(3) The observed large deuterium excess is explained, considering that the isotopic composition of initial vapor deviates from MWL toward lower $\delta^{18}O$ due to non-equilibrium evaporation on the sea surface. However, the observed deuterium excess is too large to be explained by direct applying of Merlivat and Jouzel's (1979) model.

For the formation process (condensation and sublimation processes) of cloud particles:

(4) The observed slopes of δD-$\delta^{18}O$ relation were 8.5 to 9.6 in 7 of 9 cases of graupels, snowflakes and their mixture. In the case of graupels, observed slopes are in rough agreement with that of cloud droplets calculated for isotopic equilibrium condensation. This result suggests that the value of $(\alpha_D-1)/(\alpha_{18O}-1)$ during condensation of water vapor on cloud droplets is close to that determined under isotopic equilibrium.

(5) In the case of snowflakes, the observed slopes are about 8 % greater than that calculated for isotopic equilibrium sublimation. This result can be explained by a kinetic effect due to supersaturation of water vapor in the sublimation process during growth of snow crystals shown by Jouzel and Merlivat (1984).

5 Difference of $\delta^{18}O$ of solid precipitation from a cloud between the two stations

In this section, the difference in $\delta^{18}O$ of falling snow between the two stations is mensioned. The observations described in this section were made in January 25, 14:00 - 16:30, 1986 at Ishikari plain.

5.1 Variation of $\delta^{18}O$ of solid precipitation during the lifetime of a convective cloud

The observed snowfall originated from a typical band-shaped cloud. From radar observation, the width of the band was about 10 km, and the scale of the convective clouds in it was 5 to 10 km horizontally and 2 to 2.5 km vertically. This band-shaped cloud moved in almost the same direction as its elongation, with a speed of about 35 km/h. The two stations, as shown in Fig. 2-1, were aligned about 8 km apart along the observed band-shaped cloud. Consequently, it took about 15 min for a cloud to move between them.

The intensity of snowfall observed at the leeward station during the observational period is shown in Fig. 5-1 During this period, 8 convective radar echoes passed over the leeward station; 7 of them (echoes 1 to 7 indicated in Fig. 5-1) also passed over the windward station. Snowfall from each echo was observed at the windward station about 15 min earlier than at the leeward station.

Table 5-1 shows the average values of precipitation intensity and $\delta^{18}O$ (relative to SMOW) of falling snow particles from each echo sampled at both stations. In all cases the $\delta^{18}O$ of snow particles sampled at the leeward station is smaller than that at

the windward station; the difference in $\delta^{18}O$ between the two stations ranges from 0.2 to 3.1‰. For example, the averaged value of $\delta^{18}O$ of falling snow particles from echo 2 was -13.7‰ at the windward station, and after 15 min -16.8‰ at the leeward station. The difference of $\delta^{18}O$ (3.1‰) between the two stations indicates that the $\delta^{18}O$ of snow originating from echo 2 decreases by 3.1‰ during the period of about 15 min of movement of cell over 8 km between the two stations.

Fig. 5-2 shows the intensive parts (>19dBZ) of PPI radar echoes for 7 cases during travel from the coast to the leeward station, and the RHI radar echoes of the A-A' cross section indicated in the figure for echo 1, observed at the leeward station. Judging from radar echo shapes, it is considered that each echo consists of one or two cell(s).

Factors which could cause such difference of $\delta^{18}O$ are wind direction in the cloud layer, isotopic composition of water vapor which forms the cloud, type of falling snow particles, and difference of stage of convective echo.

Radiosonde data at Sapporo at 9:00 on this day are shown in Fig. 5-3. The wind direction is almost the same in the cloud layer (< 2.5 km). Therefore, wind is not considered the reason for the difference of $\delta^{18}O$ between the two stations.

Another factor causing the difference of $\delta^{18}O$ is the isotopic composition of initial water vapor which forms the cloud. If the isotopic composition of initial water vapor for the two stations is different, it rather than precipitation process would cause the $\delta^{18}O$ variation. However, in most cases of snowfall studied here, a cloud consists of air parcels containing initial water vapor with the same isotopic composition, as described in

the previous chapter.

At both stations, the observed type of snow particles was mainly graupel pellets with diameter of about 1 mm: heavy rimed dendrites and plates were sometimes mixed in. Since no difference in the type of snow particles was observed between the two stations, type of the snow particles is apparently not responsible for the difference of $\delta^{18}O$.

Therefore, the observed difference of $\delta^{18}O$ between the two stations, shown in Table 5-1, is considered as due to the difference of stage of the cell in the convective echo. Even if the echo is multi-cellular as is echo 2, each cell is considered to drop snow particles at both stations, except for echo 4. It is reasonable, therefore, to consider that the $\delta^{18}O$ of falling snow particles from the cell decreases with time during its lifetime.

5.2 Relation between the precipitation intensity and the rate of decrease of $\delta^{18}O$

The relation between the rate of decrease of $\delta^{18}O$ and echo intensity in the windward area is examined. In the PPI echoes in Fig. 5-2, intensive parts (>24dBZ), which is blackened, are seen in the windward area in echoes 1 to 4, but not in echoes 5 to 7. Echo 3 has intensive parts in the windward area as seen in the PPI echo at 14:03 and average precipitation intensity is large at the windward station, as seen in Table 5-1, but it becomes weak during travel to the leeward station. Comparing the echo intensity in the windward area with the observed decrease of $\delta^{18}O$ in Table 5-1, a large decrease of $\delta^{18}O$ between the two stations is observed in echoes 1 to 3 which have intensive parts

in the windward area, while a small decrease is observed in weak echoes 5 to 7, except for echo 4. The decrease of $\delta^{18}O$ is the smallest in the weakest echo 7, which is underdeveloped.

Therefore, the rate of decrease of $\delta^{18}O$ of falling snow is large in a cell in which precipitation intensity is large in the windward area.

In the case of echo 4, the backward part of this echo developed suddenly after it passed over the windward station, as seen in the PPI radar echo at 14:52 in Fig. 5-2. Therefore, the precipitating cell in this echo is different between the two stations. This echo is case C described in chapter 4. As described before, the relation between δD and $\delta^{18}O$ of snow from this echo was different between the two stations; this result indicates that the isotopic composition of initial vapor which makes snow particles is different between the two stations. Therefore, the $\delta^{18}O$ of snow from this echo between the two stations should not be compared.

5.3 Relation between the stage of a cell and the rate of decrease of $\delta^{18}O$

The stage of a precipitating cell is its mature or decaying stage. In order to know the dependence of decrease of $\delta^{18}O$ on the stage of a cell, its stage in each echo will be roughly estimated from the variation of echo intensity and falling velocity of snow particles. In the cases of intensive echoes 1 to 3, the location with maximum precipitation intensity can be estimated from PPI radar echoes in Fig. 5-2.

As seen in Fig. 5-2, the PPI radar echo of echo 1 becomes intensive, as it approaches the leeward station, while in the

case of echo 2, the forward part of this echo is intensive between the two stations and the backward part is intensive near the windward station; averaging both of them, echo 2 is intensive between the windward and leeward stations. Echo 3 is intensive before the windward station. Comparing RHI radar echoes at the leeward station among echoes 1 to 3, that of echo 1 is the most intensive and those of echoes 2 and 3 are weak in turn, while the average precipitation intensity at the windward station is maximum for echo 2 as indicated in Table 5-1. From the above, it appears that maximum precipitation intensity is near the leeward station in echo 1, between windward and leeward stations in echo 2, and before the windward station in echo 3. The decrease of $\delta^{18}O$ is larger in echoes 2 and 3 in which cells are considered at a later stage than in echo 1.

The same results are obtained from the falling velocity of snow particles, as shown in Fig. 5-1. Falling velocity is observed by Doppler radar at the leeward station, and is expressed as V_s-W, where V_s is the terminal velocity of snow particles and W is the vertical velocity of the air, averaged over the height $z<2000$m, $1000<z<2000$m, or $z<1000$m. As shown in this figure, the falling velocity is about 1 m/s. Terminal velocity of observed graupel pellets is considered about 1m/s, therefore, the ascending current was considered weak if it remained in the cell, except for echo 1. The falling velocity in echo 1 is very small (about 10 cm/s) in the upper part of the cell ($1000<z<2000$m), which indicates that the ascending current remains in the upper part of the cell in echo 1 at the leeward station. There is no evidence that an ascending current

remains in echoes 2 and 3. Therefore, the stage of the cell is earlier in echo 1 than in echoes 2 and 3.

In echoes 5 to 7, since they are so weak, it is difficult to determine the location where the precipitation was the most intensive.

It can be concluded that the rate of decrease of $\delta^{18}O$ of falling snow particles is large during and after the maximum precipitation intensity in the lifetime of the cell.

6 Model of precipitation process in a convective cloud cell

The observed variation of $\delta^{18}O$ of falling snow particles indicates that vertical profiles of $\delta^{18}O$ of water vapor and snow particles in the cell vary with time. Accordingly, the variation of vertical profiles of $\delta^{18}O$ of water vapor and precipitating particles is calculated by a simple one-dimensional time-dependent cloud model which consists of a cell, simulating the growth mechanism of observed graupel pellets. This model is used to examine the relation between the rate of decrease of $\delta^{18}O$ and the effects of precipitation efficiency, convection depth and terminal velocity of the precipitating particles.

6.1 Model description

6.1.1 Basic equations

The graupel pellets grow by accretion of cloud droplets on the ice crystal. Mass growth by accretion is much greater than that by sublimation (deposition). Then, as water in a cell, water vapor, cloud droplets and solid particles which include both ice crystals and falling snow particles (graupels) are considered. In order to simplify the model, it is assumed that water vapor and cloud droplets move with the air, and the only three microphysical processes which are essential are considered, that is, the condensation of water vapor to cloud droplets, conversion (glaciation) of cloud droplets to ice crystals and accretion of cloud droplets to solid particles. Sublimation and evaporation processes are not considered here.

The dynamic model used here is essentially the same as the one-and-a-half-dimensional model developed by Asai and Kasahara (1967) and Ogura and Takahashi (1971). In this model, a

convective cloud cell is cylindrical with time-independent radius A, which is assumed as 3 km here. All equations are one-dimensional in space; cloud variables are averaged over the horizontal cross-section of the cloud. However, the radial component of velocity is considered to evaluate entrainment.

Assuming that pressure and density of the air in the cloud approximately equal to those of environment, the vertical component of the equation of the motion is written in the cylindrical coodinates (r, λ, z) as;

$$\rho\frac{\partial w}{\partial t} + \frac{1}{r}\frac{\partial}{\partial r}(\rho ruw) + \frac{1}{r}\frac{\partial}{\partial \lambda}(\rho vw) + \frac{\partial}{\partial z}(\rho ww) = \rho g\frac{T_v - T_{ve}}{T_{ve}} \qquad (6\text{-}1)$$

where u, v, w are the radial, tangential and vertical components of the velocity, T_v is the virtual temperature, g the acceleration of gravity, ρ dry air density and subscript e means environment.

The equation of mass continuity is written as;

$$\frac{1}{r}\frac{\partial}{\partial r}(\rho ru) + \frac{1}{r}\frac{\partial}{\partial \lambda}(\rho v) + \frac{\partial}{\partial z}(\rho w) = 0 \qquad (6\text{-}2)$$

Integrating the Eq. (6-1) over the cross-section of the cloud, following equation is derived;

$$\frac{\partial w}{\partial t} + \frac{2}{A}(\tilde{u}_a\tilde{w}_a + \widetilde{u''_a w''_a}) + \frac{1}{\rho}\frac{\partial}{\partial z}\{\rho(\bar{w}\,\bar{w} + \overline{w'w'})\} = g\frac{\bar{T}_v - T_{ve}}{T_{ve}} \qquad (6\text{-}3)$$

where for any variables

$$\left.\begin{aligned} B &= \frac{1}{\pi A^2}\int_0^{2\pi}\int_0^{A} B\, r\, dr\, d\lambda \\ B_a &= \frac{1}{2\pi}\int_0^{2\pi} B\, d\lambda \qquad \text{at} \quad r = A \\ \bar{B} &= B - B', \quad \text{and} \quad \tilde{B}_a = B - B''_a \end{aligned}\right\} \qquad (6\text{-}4)$$

In Eq. (6-3), the term $\widetilde{u''_a w''_a}$ represents the lateral eddy excahnge of momentum between the cloud and environment. Following to Ogura and Takahashi (1971), $\widetilde{u''_a w''_a}$ is assumed as

$$\widetilde{u''_a w''_a} = \gamma^2 |w| w,$$

and ignoring the term $\overline{w' w'}$ and adding the drag force, the equation for vertical velocity W (m/s) is written as follows;

$$\frac{\partial W}{\partial t} = - W\frac{\partial W}{\partial z} - \frac{2}{A}\gamma^2 W|W| + \frac{2}{A} U_a (W - W_a) + g \frac{T_v - T_{ve}}{T_{ve}} - g (Q_c + Q_s) \qquad (6\text{-}5)$$

where $W = \overline{w}$, $U_a = \widetilde{u}_a$, $W_a = \widetilde{w}_a$ and the other bar symbol is omitted. The virtual temperature T_v is calculated from $T(1+0.608Q_v)$, and T temperature; Q_v, Q_c and Q_s are mixing ratios (g/g) of water vapor, cloud droplets and solid particles. The value of parameter γ^2 used here is 0.1, according to Ogura and Takahashi (1971).

In Eq. (6-5), five terms in the right hand side are vertical advection, lateral eddy exchange, dynamic entrainment, buoyancy and drag force.

The value of U_a is calculated from the mass continuity equation, which is obtained by similar integration of Eq. (6-2):

$$\frac{2}{A} U_a + \frac{1}{\rho}\frac{\partial}{\partial z}(\rho W) = 0 \qquad (6\text{-}6)$$

Similarly, the thermodynamic equation is written as

$$\frac{\partial T}{\partial t} = - W\frac{\partial T}{\partial z} - \Gamma_d W + \frac{2}{A}\gamma^2 |W| (T_e - T) + \frac{2}{A} U_a (T - T_a) + \frac{L_c}{C_p} P_1 + \frac{L_f}{C_p} (P_2 + P_3) \qquad (6\text{-}7)$$

where T is air temperature, Γ_d dry adiabatic lapse rate, C_p

specific heat of air, L_c and L_f are latent heat of condensation and freezing, and P_1 is rate of condenstion. P_2 and P_3 are rate of conversion (glaciation) of cloud droplets to ice crystals and rate of stochastic growth of graupels by accretion of cloud droplets, as follows:

$$P_2 \text{ (conversion)} = k_2 Q_c \tag{6-8}$$

$$P_3 \text{ (accretion)} = k_3 Q_c Q_s \tag{6-9}$$

The value of parameter k_3 used here is 2, and the values of k_2 is listed in Table 6-1.

In order to calculate the isotopic composition, equations of mass continuity are formulated here for water vapor, cloud droplets and solid particles:

$$\frac{\partial Q_v}{\partial t} = -\frac{1}{\rho}\frac{\partial}{\partial z}(\rho W Q_v) - \frac{2}{A}U_a Q_{va} + \frac{2}{A}\gamma^2 |W|(Q_{ve} - Q_v) - P_1 \tag{6-10}$$

$$\frac{\partial Q_c}{\partial t} = -\frac{1}{\rho}\frac{\partial}{\partial z}(\rho W Q_c) - \frac{2}{A}U_a Q_{ca} - \frac{2}{A}\gamma^2 |W| Q_c + P_1 - P_2 - P_3 \tag{6-11}$$

$$\frac{\partial Q_s}{\partial t} = -\frac{1}{\rho}\frac{\partial}{\partial z}(\rho W Q_s) - \frac{2}{A}U_a Q_{sa} - \frac{2}{A}\gamma^2 |W| Q_s + P_2 + P_3 \tag{6-12}$$

and for their isotopes;

$$\frac{\partial}{\partial t}(Q_v R_v + Q_c R_c) = -\frac{1}{\rho}\frac{\partial}{\partial z} W(Q_v R_v + Q_c R_c) - \frac{2}{A}U_a(Q_{va}R_{va} + Q_{ca}R_{ca}) + \frac{2}{A}\gamma^2 |W|(Q_{ve}R_{ve} - Q_v R_v - Q_c R_c) - R_c(P_2 + P_3) \tag{6-13}$$

$$R_c = \alpha R_v$$

$$\frac{\partial}{\partial t} Q_s R_s = -\frac{1}{\rho}\frac{\partial}{\partial z}(W - V_s) Q_s R_s - \frac{2}{A} U_a Q_{sa} R_{sa} - \frac{2}{A}\gamma^2 |W| Q_s R_s + R_c(P_2 + P_3) \tag{6-14}$$

where R_v, R_c and R_s are isotopic ratios ($H_2{}^{18}O/H_2{}^{16}O$) for vapor, cloud droplets and solid and α is the isotope fractionation

factor, for which the value determined by Majoube (1971) is used here, and V_s is the terminal velocity of the solid. According to Ogura and Takahashi (1971), V_s (m/s) is written as

$$V_s = 3.12 \left(\rho Q_s \right)^{0.125} f_o \qquad (6\text{-}15)$$

where f_o is 0.75 for hailstones and 0.37 for graupel pellets. The value of 0.37 is used for comparison of calculated results with observational results, for which V_s is about 1 m/s.

The following assumptions are made to formulate the equations on isotopes; 1) isotopic composition of cloud droplets is in equilibrium with that of water vapor; 2) there is no isotope fractionation during conversion and accretion of cloud droplets to solid, namely fractional freezing does not occur.

The quantities at cloud perimeter (W_a, T_a, Q_{va}, etc.) are assumed as follows; for any variables B_a,

$B_a = B$, if $U_a > 0$ (outflow), and

$B_a = B_e$, if $U_a < 0$ (inflow).

The intensity of snowfall is calculated as flux of solid at the surface, namely, $3.6 \rho Q_s V_s$ (mm/h).

6.1.2 Environment, initial and boundary conditions

The lapse rate of environmental air was assumed to be 0.83 °C/100m which was the observed value under the inversion layer, as shown in Fig. 5-3. The observed convective clouds developed on the relatively warm sea surface. Then, the superadiabatic lapse rate (1.03, 1.33 or 1.83 °C/100m) is assumed at the bottom layer of the air during development of the cell (10 or 30 min). Relative humidity is assumed to be 100 % at the surface and to decrease with height to 50 % at 5 km. In the environmental air, W, Q_c and Q_s are assumed to be zero.

The $\delta^{18}O$ of the initial vapor is needed to compare the value of $\delta^{18}O$ between calculation and observation. However, since comparison of the rate of decrease of $\delta^{18}O$ is the essential point here, the $\delta^{18}O$ value is expressed as the per mille deviation from the isotopic ratio of initial water vapor (R_{vo}), namely:

$$\delta^{18}O \text{ (relative to initial vapor)} = \frac{R - R_{vo}}{R_{vo}} \times 1000 \ (‰) \qquad (6\text{-}16)$$

The $\delta^{18}O$ values of water vapor ($\delta^{18}O_v$), cloud droplets ($\delta^{18}O_c$) and solid ($\delta^{18}O_s$) are calculated from the above. In this chapter, the calculated $\delta^{18}O$ is the value relative to initial vapor, unless "SMOW" is added.

The vertical gradient of $\delta^{18}O$ of water vapor with height is unknown here, however, its effect is small. For example, the assumption of gradient -0.3‰/100m of $\delta^{18}O_v$ gives only a 10 % larger rate of decrease of $\delta^{18}O$ of falling snow. Therefore, an isotopically homogeneous environment is assumed.

The boundary conditions are W=0, $T=T_e$, water vapor saturated, $R_v=R_{vo}$ and $Q_c=0$ at the surface. Initial condition were assumed to be the same as the environment, except in the layer z = 100 m to 1 km where an excess temperature +0.5°C was given as the initial disturbance.

6.1.3 Computational scheme and calculated cases

The method for calculation used here is a "forward-upstream" scheme. The space differentials are transformed to finite differences between the considered level and upstream level, using grid points as shown in Fig. 6-1. The space increment is 100 m and time increment is 5 seconds. For the value of W in the advection term in equation (6-5), the averaged value over

three points, one below and one above the considered grid point is used. If W becomes negative, it is assumed zero to exclude non-essential oscillation.

The procedure of the calculation is similar to that of Ogura and Takahashi (1971). For isotope calculation, it is assumed that, among the three microphysical processes considered here, condensation of vapor to cloud droplets takes place first, and conversion and accretion of cloud droplets to solid are second.

The calculations were done for 25 cases with different parameters k_2 for precipitation efficiency, f_o for terminal velocity of solid and lapse rate at the bottom layer of air. Among these cases the following 4 cases indicated in Table 6-1 will be described in detail: the standard case (R1), the case of relatively low precipitation efficiency (R2), and the case of relatively shallow convection (R3). In these cases the precipitating particles are graupel pellets of which terminal velocity is relatively small, except in R4 in which case they have larger terminal velocity.

6.2 Calculated results

6.2.1 Vertical profiles of $\delta^{18}O$ of water vapor and graupels

The variation of vertical profiles of calculated values during the lifetime of a cell for the standard case R1 will be described in this section. Case R1 is considered to be close to observed snowfall. The results are shown in Fig. 6-2. Snow particles grow in the updraft and start to fall after the acsending current becomes weak, as shown in the time-height cross section of vertical velocity (W) and mixing ratio of solid

particles (Q_s) in Fig. 6-2a and b. The $\delta^{18}O$ of water vapor ($\delta^{18}O_v$) varies with development of the cell, as shown in Fig. 6-2d. The minimum value of $\delta^{18}O_v$ is -13.0‰ at a height of 2.9 km (gradient -0.45‰/100m) at time 40 min when the cell is most highly-developed.

The vertical $\delta^{18}O_v$ gradient by this model are smaller than those obtaineded from the δD gradient calculated by Federer et al. (1982a) and Rozanski and Sonntag (1982). The precipitating particles are solid in this model, so they do not exchange isotopes with vapor, while raindrops exchange isotopes with vapor in their model. Adding to this, the updraft becomes weak due to the drag force of particles if the cloud is not steady-state, while water vapor with low $\delta^{18}O$ due to exchange of isotopes continues to ascend in their steady-state model.

The vertical profile of $\delta^{18}O$ of solid particles ($\delta^{18}O_s$) varies with time as seen in Fig. 6-2e. Its gradient at the time 40 min is the largest (about 1‰/100m) at 2.6 km height where the solid particles accumulate in the ascending current, as seen in this figure. After the updraft becomes weak, these accumulated solid particles start to fall, so the vertical gradient of $\delta^{18}O_s$ becomes small. Consequently, the $\delta^{18}O_s$ at the surface decreases with time; the rate of decrease is large while the precipitation intensity is large, as shown in Fig. 6-2f. The maximum decrease of $\delta^{18}O_s$ during 15 min is 3.0‰.

6.2.2 Dependence of the rate of decrease of $\delta^{18}O$ on the various factors

Fig. 6-3 shows the time variation of $\delta^{18}O$ of falling snow ($\delta^{18}O_s$) at the surface for R2 to R4, and Fig. 6-2f does that for

R1. From these figures, the more intensive the precipitation, the larger the rate of decrease of $\delta^{18}O_s$. The maximum decrease of $\delta^{18}O_s$ during 15 min for each case is 1.8 to 4.6‰ as indicated in Table 6-1.

i) Efficiency of precipitation

Comparing case R2 with R1, the dependence of the rate of decrease of $\delta^{18}O_s$ on precipitation efficiency is examined. The difference of condition between R2 and R1 is expressed parameter k_2 in equation (6-8), as shown in Table 6-1. In case R2, since k_2 is small, the rate of conversion from cloud droplets to solid is small, so the mixing ratio of cloud droplets (Q_c) is larger than in case R1; namely, precipitation efficiency in R2 is lower than in R1. The rate of decrease of $\delta^{18}O$ in case R2 with low precipitation efficiency is smaller than in R1.

Such a difference in the rate of decrease is caused by the difference in the vertical profiles of $\delta^{18}O_v$ and $\delta^{18}O_s$ as seen in Fig. 6-4. At 40 min, $\delta^{18}O_v$ in case R2 with low precipitation efficiency is slightly larger than in R1 in the upper part of the cell, because cloud droplets act as a buffer to decrease the vertical gradient of $\delta^{18}O_v$. The $\delta^{18}O_s$ in R2 is, therefore, larger than in R1 at this time in upper part, where the solid particles accumulate as seen in Fig. 6-2e. Consequently, the rate of decrease of $\delta^{18}O_s$ at the surface in R2 is smaller than in R1, although the difference in $\delta^{18}O_v$ between them is slight.

The $\delta^{18}O$ of falling snow decreases greatly in a cell in which cloud droplets are converted to snow particles effectively.

ii) Depth of convection

In case R3, lapse rate at the bottom air layer is small; consequently the ascending current is weak and the cloud top is

lower than other cases, as indicated in Table 6-1. The minimum value of $\delta^{18}O_v$ is -7.4‰ at 2.1 km height; consequently, the vertical gradients of $\delta^{18}O_v$ and of $\delta^{18}O_s$ are small. Therefore, in an underdeveloped cell as in case R3, the rate of decrease of $\delta^{18}O_s$ is small, as shown in Fig. 6-3b.

iii) Falling velocity of precipitating particles

The effect of falling velocity of snow is examined by comparing R4 with other cases. Terminal velocity of the solid particles V_s is the value for hailstones (about 2 m/s) in R4 and for graupel pellets (about 1 m/s) in other cases. Since large particles are formed in a intensive updraft, large superadiabatic lapse rate at bottom air layer is assumed in R4. In this case, solid particles with low $\delta^{18}O_s$ which grow in the higher part of the cloud reach the surface earlier because of large falling velocity.

Therefore, the rate of decrease of $\delta^{18}O_s$ is large when the falling velocity of precipitating particles is large. The same is true for a cell precipitating raindrops of large terminal velocity.

6.2.3 The effect of amount of precipitation on the $\delta^{18}O$ of solid precipitation

As seen in Fig. 6-2f and Fig. 6-3, the $\delta^{18}O_s$ at the beginning of precipitation is similar in all cases, namely about 12‰; in addition the rate of decrease of $\delta^{18}O_s$ is large in a cell in which the precipitation intensity is large. Therefore, it is expected that the $\delta^{18}O_s$ is related to the amount of precipitation from the cell.

The relation between total amount of precipitation from a

cell and the $\delta^{18}O_s$ in the last stage of the cell calculated from 25 cases is shown in Fig. 6-5. The values of parameters in these cases are 0.0002 to 0.002 for k_2 and 0.37 or 0.75 for f_o, and lapse rate at the bottom air layer is 0.83 to 1.83°C/100m during the period of 0 to 30 min. As seen in Fig. 6-5, $\delta^{18}O_s$ is smaller in the last stage of a cell which has dropped more precipitation. The $\delta^{18}O$ in any stage of each cell decreases with time during its lifetime. Therefore, at any stage in the lifetime of a cell the smaller $\delta^{18}O$, the more precipitation has fallen from the cell before.

7 Comparison between observed and model results

As described in the previous chapter, the decrease of $\delta^{18}O$ of falling snow particles during the lifetime of a cell was shown by the model. Therefore, the observed decrease in $\delta^{18}O$ between the two stations can be explained on the basis of decrease of $\delta^{18}O$ during the lifetime of the cell. Even in the case of a multi-cellular convective echo, the $\delta^{18}O$ of snow from each echo decreases with time. Accordingly, the observed difference is interpreted as the decrease of $\delta^{18}O$ averaged over both cells, since each cell drops snow at both stations, except for echo 4.

The calculated rate of decrease of $\delta^{18}O$ is large in a cell with large precipitation intensity. This result agrees with observation as described in 5.2.

For an underdeveloped cell, the calculated result for R3 also agrees with observation for echo 7, that is, the rate of decrease of $\delta^{18}O$ is very small.

From the model calculation, the rate of decrease of $\delta^{18}O$ is large while the precipitation intensity is large, as seen in Fig. 6-2f as described in 6.2.1. The observed rate of decrease is maximum in echo 2 in which location of maximum precipitation intensity is between windward and leeward stations. This observational result agrees with the calculated result.

However, in the model calculation the rate of decrease of $\delta^{18}O$ becomes small at the stage of the cell after its maximum precipitation intensity, while the large rate of decrease of $\delta^{18}O$ (3.0‰) is also observed in echo 3 in a later stage than for echo 2.

Such disagreement is considered to be due to different

dynamical process. In a one-dimensional model, precipitating particles fall out through the same cross-section of the cell as the updraft. Consequently, vertical velocity (W) becomes small and vanishes at all heights of the cell during a short period, as seen in Fig. 6-2a. In addition, in this model W is assumed zero if it becomes negative, while, in an actual cell the ascending current remains in part of the cell while downdraft develops in the rest of the cell. If this condition continues, the large decrease of $\delta^{18}O$ of snow continues until the last stage of the cell. Such a condition cannot be expressed in this model. Echoes 2 and 3 were possibly in such a condition before they reached the leeward station.

Isotopic processes in a single cell are discussed above; however, for further discussion, it is necessary to consider the isotopic processes in a cloud system. In that case, the isotopic composition of initial water vapor which makes a cloud is the most important problem.

If water vapor with low $\delta^{18}O$ which have previously produced precipitation recycle into another new cell again in a cloud system, the initial water vapor of the new cell has smaller $\delta^{18}O$ than that of the previous cell, but the same δD-$\delta^{18}O$ relation as the previous cell. If such a recycle process of water vapor and cloud water occurs, the precipitation from a new cell has smaller $\delta^{18}O$, but the same δD-$\delta^{18}O$ relation.

The smallest average $\delta^{18}O$, as seen in Table 5-1, was observed in echo 3 of which stage is the latest among echoes 1 to 3. This variation of average $\delta^{18}O$ from echoes 1 to 3 can be explained by the model results. However, to discuss this variation quantitatively, one needs to know the $\delta^{18}O$ of initial

water vapor, considering the isotopic process in the cloud system, as mensioned above.

In the case of echo 4, since the precipitating cell at the leeward station in echo 4 was newly developed, $\delta^{18}O$ of snow from echo 4 at the leeward station was expected to be larger than that at the windward station, if the $\delta^{18}O$ of initial vapor of the cell was the same as previous cell. However, $\delta^{18}O$ at the leeward station was smaller than that at the windward station, though the difference between them was small. Adding to this, the δD-$\delta^{18}O$ relation is different between them. These indicates that mixture of recycled water vapor with low $\delta^{18}O$ and water vapor with different δD-$\delta^{18}O$ relation possibly made the new cell.

Follows are concluded on the precipitation process from the observed isotopic difference between the two stations and numerical modeling.

(1) The $\delta^{18}O$ of the falling snow particles from a convective cloud decreases with time during its lifetime. The rate of decrease observed in 7 cases of convective radar echoes was 0.2 to 3.1‰ during 15 min of movement between two stations; the rate was large during and after its maximum precipitation intensity in the lifetime.

(2) A large rate of decrease of $\delta^{18}O$ was observed in cells in which precipitation intensity has been large in the windward area; a very small decrease (0.2‰) was observed in an underdeveloped cell.

The one-dimensional and time-dependent model presented here can explain the observed results well, except for the fact that a large rate of decrease of $\delta^{18}O$ was observed in the cell after its

maximum precipitation intensity. The following conclusions are also drawn from the model results.

(3) The rate of decrease of $\delta^{18}O$ is large in cells in which cloud droplets are effectively converted to ice crystals in it, in cells which is well-developed and in cells in which terminal velocity of precipitating particles is large.

(4) The smaller $\delta^{18}O$ of falling snow particles from a cell, the more precipitation has fallen from the cell before.

8 Conclusion

Observations at two stations along the cloud trajectory and modeling were done on the isotopic composition of solid precipitation from a convective cloud during the winter monsoon on the Ishikari plain and Hokuriku district, Japan. The following conclusions are drawn on the behavior of water isotopes in the precipitation process.

The δD and $\delta^{18}O$ values of falling snow particles produced in a separate cloud or a radar echo have a linear relationship. It can be concluded from such linearity that a cloud which produces falling snow particles observed at these two stations consistes of air parcels containing initial water vapor with the same isotopic composition. The observed values of deuterium excess were much greater than 10, and they differed from case to case. The variations of deuterium excess indicate that the isotopic composition of initial water vapor constituting a cloud differs from case to case, namely the isotopic composition of water vapor constituting clouds varies with time.

The fractionation during evaporation (including upward transportation) of water vapor from the the sea surface can be discussed from the values of deuterium excess. The observed large values of deuterium excess indicate that non-equilibrium fractionation occurs during evaporation of water vapor from the sea surface. The observed deuterium excess is too large to be explained by direct application of Merlivat and Jouzel's (1979) model. The kinetic effect during evaporation should be modeled, including more effective fractionation during transportation by turbulence as discussed by Craig and Gordon (1965).

Linearity between δD and $\delta^{18}O$ values of snow from a cloud made it possible to discuss the fractionation during condensation and sublimation from the slope of the δD-$\delta^{18}O$ relation. The observed slopes of the δD-$\delta^{18}O$ relation were 8.5 to 9.6 in 7 of 9 cases of graupels, snowflakes and their mixture. In the case of graupels, observed slopes roughly agree with that of cloud droplets calculated for isotopic equilibrium condensation. This result suggests that the value of $(\alpha_D-1)/(\alpha_{18O}-1)$ during condensation of water vapor on cloud droplets is close to that determined by Majoube (1971) under isotopic equilibrium.

In the case of snowflakes, the observed slopes are about 8 % greater than that calculated for isotopic equilibrium sublimation. Consequently, the value of $(\alpha_D-1)/(\alpha_{18O}-1)$ during sublimation is close to that during condensation. This result can be explained by a kinetic effect due to supersaturation of water vapor in the sublimation process during growth of snow crystals shown by Jouzel and Merlivat (1984).

The constancy of the isotopic composition of initial water vapor in a cloud also made it possible to know the $\delta^{18}O$ variation of solid precipitation during the lifetime of a convective cloud. The $\delta^{18}O$ of graupel pellets from a convective cloud decreases with time during its lifetime. The rate of decrease observed in 7 cases of convective radar echoes was 0.2 to 3.1‰ during 15 min of movement between two stations; the rate was large during and after its maximum precipitation intensity in the lifetime. A large rate of decrease of $\delta^{18}O$ was observed in cells in which precipitation intensity was large in the windward area; a very small decrease (0.2‰) was observed in an

underdeveloped cell.

The one-dimensional and time-dependent model simulating a graupel bearing convective cloud cell presented here can explain the observed results well, except for the fact that a large rate of decrease of $\delta^{18}O$ was observed in the cell after its maximum precipitation intensity.

The model results also show that the rate of decrease of $\delta^{18}O$ is large in cells in which cloud droplets are effectively converted to ice crystals, in cells which are well-developed and in cells in which terminal velocity of precipitating particles is large, consequently, in cells in which precipitation is intensive. Accordingly, the more precipitation that has fallen from a cell, the smaller the $\delta^{18}O$ of falling snow particles from the cell.

The precipitation mechanism differs from cloud to cloud. However, the fractionation during condensation and sublimation are the same as that concluded in this study. In addition, the isotopic composition can be calculated in various models such as cloud models and GCMs in a way similar to that used in the present study, since the isotopic composition has no feedback to the dynamic process.

For the purpose of understanding various interesting facts on the isotopic composition of precipitation which have been observed, it is necessary to consider the isotopic composition of initial water vapor which makes a cloud and the isotopic process in a cloud system.

In the case of a convective cloud of relatively small scale, the isotopic composition of the initial water vapor is considered constant. However, the isotopic composition of water vapor

constituting clouds varies with time over several hours. Such variation of the isotopic composition of initial water vapor has not been considered in most previous studies. In addition, the δD and $\delta^{18}O$ of water vapor become small along the δD-$\delta^{18}O$ line during the precipitation process. Accordingly, the δD and $\delta^{18}O$ in a cloud system possibly become smaller than that in an isolated cloud by recycling of water vapor with low δD and $\delta^{18}O$.

Hourly variations between the surface air temperature and $\delta^{18}O$ of snow was observed to be correlated in Hokuriku. Such a correlation is considered to be caused by the variation in the isotopic composition of initial water vapor constituting clouds and the stage of the convective cloud at the time of landfall.

For discussion of the monthly or annual mean values, it is necessary to clarify the isotopic composition of precipitation from stratiform clouds associated with synoptic disturbances. In the case of a stratiform cloud, among the isotopic processes in the cloud, fractionation during condensation and sublimation are the same as in a convective cloud. The δD and $\delta^{18}O$ of initial water vapor constituting a stratiform cloud, however, possibly change with time and space, since ascending current lasts a long time and the horizontal scale of the cloud is large.

From the results of this study, the non-linearity between δD and $\delta^{18}O$ of precipitation associated with a warm front shown to exist by Gedzelman and Lawrence (1982) is considered to be caused by the variation of the isotopic composition of initial water vapor.

The monthly or annual mean values of $\delta^{18}O$ at a station are the results of averaging over all precipitation from various

types of clouds which pass over the station at various stages.

It is important to consider the geographical $\delta^{18}O$ distribution of precipitation with various scales.

Within the distance which a convective cloud can move during its lifetime, the isotopic variation of precipitation with time can be considered a variation with space. The maximum rate of decrease of $\delta^{18}O$ observed with distance in the present study was 3.1 ‰/ 8 km. This rate is two orders of magnitude larger than that observed as the "continental effect" or the "latitude effect". The difference in type of precipitation and precipitation mechanism with area should be considered.

For the purpose of understanding the mean values and the global scale distribution, it is necessary to not only study the correlation between the isotopic composition of precipitation and other factors such as temperature, but also to observe the isotopic compositions of water vapor and precipitation and to model the transportation of water vapor and the precipitation process isotopically using GCMs. In that case, the isotopic process in a cloud system should be taken into consideration in the isotopic parameterization of sub-grid scale cumulus convection.

For this purpose, the next step is to understand the isotopic processes in a cloud system and to clarify the mechanism of the variation of the isotopic composition of initial water vapor.

Table 4-1. Characteristics of the samples used in this chapter

Case	station[*1]	region		sampling (JST)	type[*2]	P_{av}[*3] mm/hr	hight of echo top[*4] km	surface air temperature °C
A	w	Ishikari p.	1986.1.25	13:55-14:02	g	2.8	2.2	
	l			14:02-14:18	g	2.2		-6.5
B	w			14:13-14:27	g	2.6	1.6	
	l			14:25-14:44	g	0.31		-6.5
C	w			14:27-14:55	g	2.9	2.0	
	l			14:44-15:03	g	1.7		-6.5
D	l	Ishikari p.	1986.1.28	14:35-16:00	g+ns	1.4	1.9	-6.0
E	l		1986.2.6	18:30-19:31	ns	1.7	2.0	-5.5
F	l		1985.1.30	13:37-14:17	g+rs	1.3	2.5	-9.0
G	w	Hokuriku	1983.2.7	8:40-9:45	g+rs	2.2	4<<	0
	l			9:30-11:00	rs	2.1	<6	
H	w			16:20-17:50	g+rs	3.5	4<<	0
	l			17:00-18:00	rs	2.0	<6	
I	w			18:10-19:20	rs	0.77	2<<	0
	l			18:30-22:00	rs	0.97	<4	

*1 station w: windward station, l: leeward station

*2 type of falling snow particles;

g: graupel, ns: non-rimed snowflake, rs: rimed snowflake

*3 Average intensity of precipitation was calculated from the amount of precipitation divided by sampling duration.

*4 In Ishikari plain, radar observations were made at the leeward sampling station with short range RHI, while in Hokuriku, they were made with PPI digital radar by the Japan Meteorological Agency at Fukui, 50 km WNW of the windward sampling station.

Table 4-2. Slope (s) and intercept (d) of δD-$\delta^{18}O$ line observed

Case	region	date	type*1	s*2	d*2
A	Ishikari p.	1986.1.25	g	9.6	65
B			g	9.2	60
C			g	9.6(7.4)	65(34)
D		1986.1.28	g+ns	9.4	71
E		1986.2.6	ns	9.3	54
F		1985.1.30	g+rs	9.5	59
G	Hokuriku	1983.2.7	g+rs	8.5	30
H			g+rs	9.4	47

*1 As in Table 4-1.

*2 Regression line was expressed as $\delta D = s\ \delta^{18}O + d$. In case C values were calculated from data points on the first line; those in ( ) were calculated from all data points.

Table 4-3. Comparison of the observed slope (s) and the calculated slope assuming the isotopic equilibrium (s_{eql} and s_{eqs})

case	type*1	s	s_{eql}*2 (liquid)	s_{eqs}*3 (solid)	δD_v^0 ‰	$\delta^{18}O_v^0$*4 ‰	initial temperature °C
A	g	9.6	9.2		-100	-17.9	-11
B	g	9.2	9.2		-100	-17.9	-11
C	g	9.6	9.2		-100	-17.9	-11
D	g+ns	9.4	9.2	8.7	-101	-18.8	-11
E	ns	9.3	9.1	8.6	-100	-17.0	-10
F	g+rs	9.5	9.4	8.8	-100	-17.1	-13
G	g+rs	8.5	8.7	8.3	-92	-14.6	-3
H	g+rs	9.4	8.8	8.3	-92	-15.2	-4

*1 As in Table 4-1

*2 s_{eql}(liquid) is the slope of the δD-$\delta^{18}O$ relation of cloud droplets calculated for isotopic equilibrium between liquid and vapor.

*3 s_{eqs}(solid) is the slope for ice crystals calculated for isotopic equilibrium between solid and vapor.

*4 The values of δD_v^0 and $\delta^{18}O_v^0$ are the isotopic compositions of initial vapor which are estimated by means of the method shown in Fig. 3-3 on assumption of the sea surface temperature of 5°C for the cases obtained in Ishikari plain and 10°C for those in Hokuriku.

Table 5-1. Observations.

Average valeus of $\delta^{18}O$ of falling snow particles from echoes 1 to 7 observed at windward station (w) and at leeward station (1).

echo	sampling time w	sampling time 1	average precipitation intensity (mm/h) w	average precipitation intensity (mm/h) 1	average $\delta^{18}O$ (SMOW ‰) w	average $\delta^{18}O$ (SMOW ‰) 1	difference of $\delta^{18}O$ (‰)
1	13:55-14:02	14:02-14:18	2.8	2.2	-13.2	-14.5	1.3
2	14:02-14:13	14:18-14:25	4.6	1.2	-13.7	-16.8	3.1
3	14:13-14:27	14:25-14:44	2.6	0.3	-14.7	-17.7	3.0
4	14:27-14:55	14:44-15:03	2.9	1.7	-14.5	-15.4	0.9
5	14:55-15:14	15:03-15:30	2.0	0.5	-14.0	-15.1	1.1
6	15:14-15:31	15:30-15:41	1.9	1.8	-13.2	-13.7	0.5
7	15:52-16:04	16:03-16:25	0.8	0.3	-12.8	-13.0	0.2

Table 6-1. Model Calculations.

The values of parameters and calculated maximum height of cloud, maximum precipitation intensity and maximum decrease of $\delta^{18}O$ during 15 min in each case.

case	parameters k_2	parameters f_o	lapse rate at bottom air layer (°C/100m)	lapse rate at bottom air layer (min)	max. height (km)	max.prec. intensity (mm/h)	max.decrease of $\delta^{18}Os$ (‰/15min)
R1	0.001	0.37	1.33	30	3.1	4.1	3.0
R2	0.0002	0.37	1.33	30	2.8	2.3	2.5
R3	0.001	0.37	1.03	10	2.4	1.9	1.8
R4	0.001	0.75	1.83	30	3.4	10.2	4.6

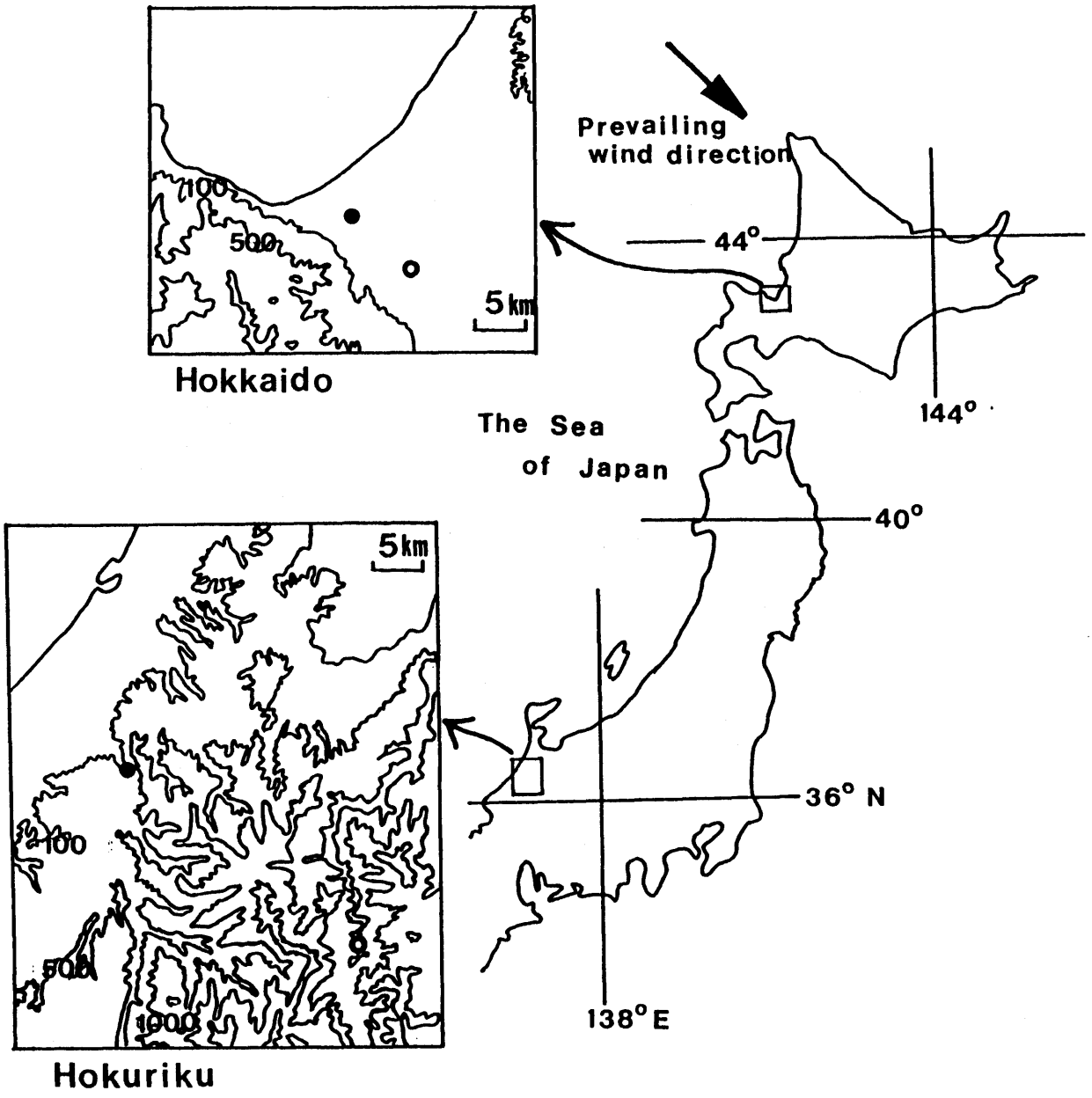

Fig. 2-1 Localities of sampling stations in Ishikari plain, Hokkaido and Hokuriku, Japan. In each area, the observations were carried out at two stations: windward station (closed circles) and leeward station (open circles). Contour lines indicate height above sea level (m)

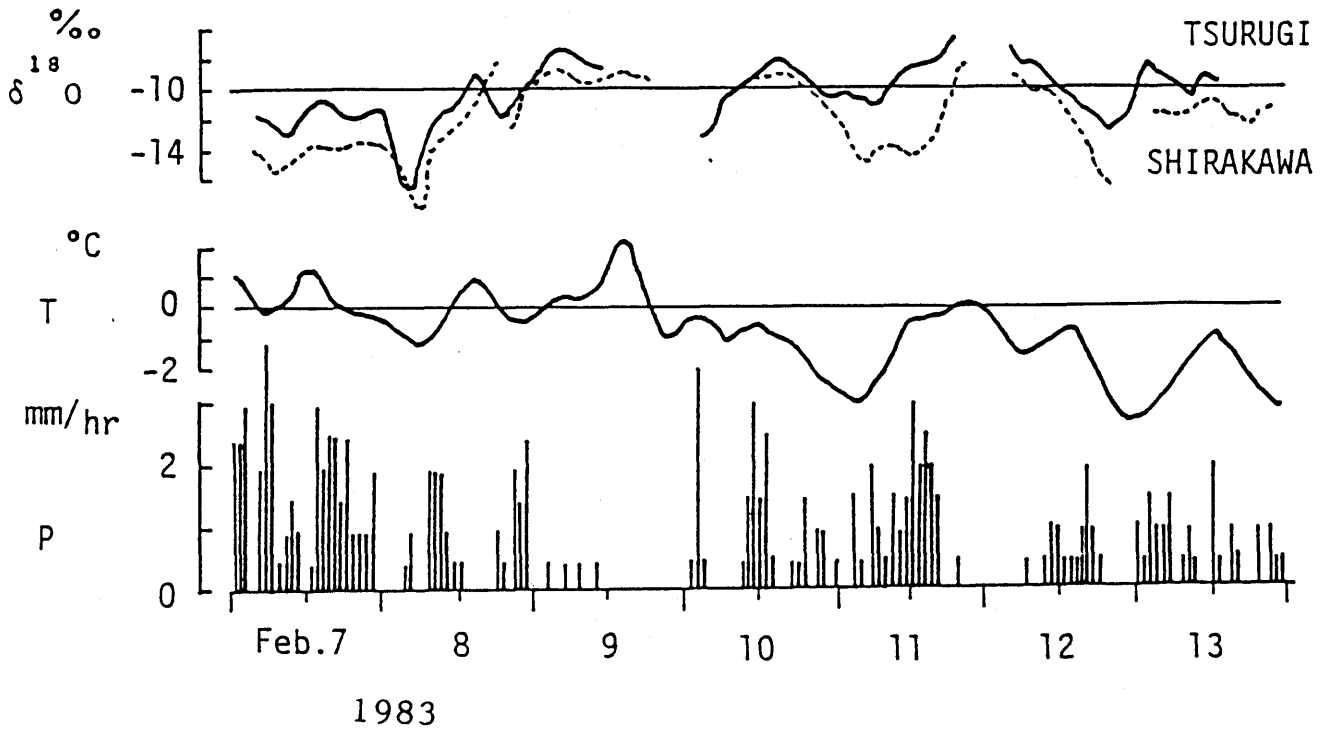

Fig. 3-1 Variations of 6 hours running mean $\delta^{18}O$ of falling snow observed at windward station, Tsurugi, (solid line) and at leeward station, Shirakawa, (broken line) and of surface air temperature and hourly precipitation at Tsurugi.

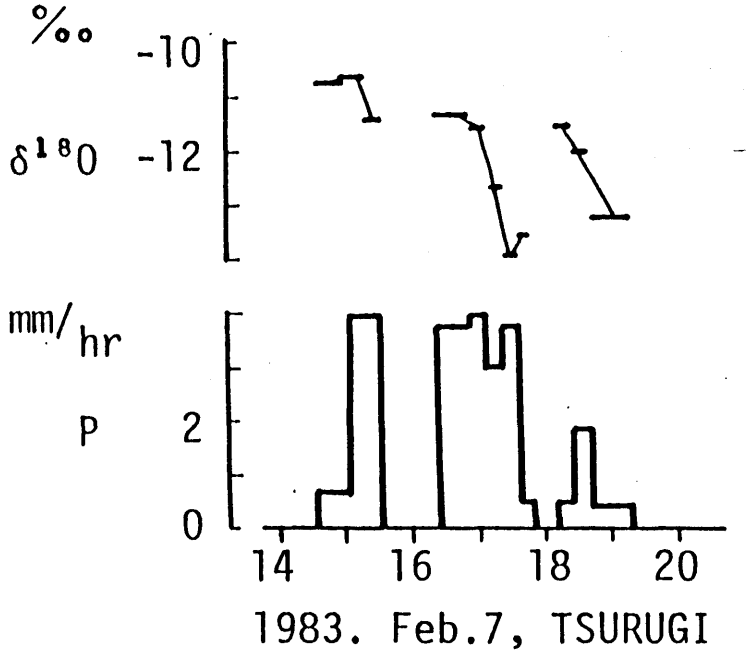

Fig. 3-2 Variation of $\delta^{18}O$ and precipitation intensity during a passage of a cloud.

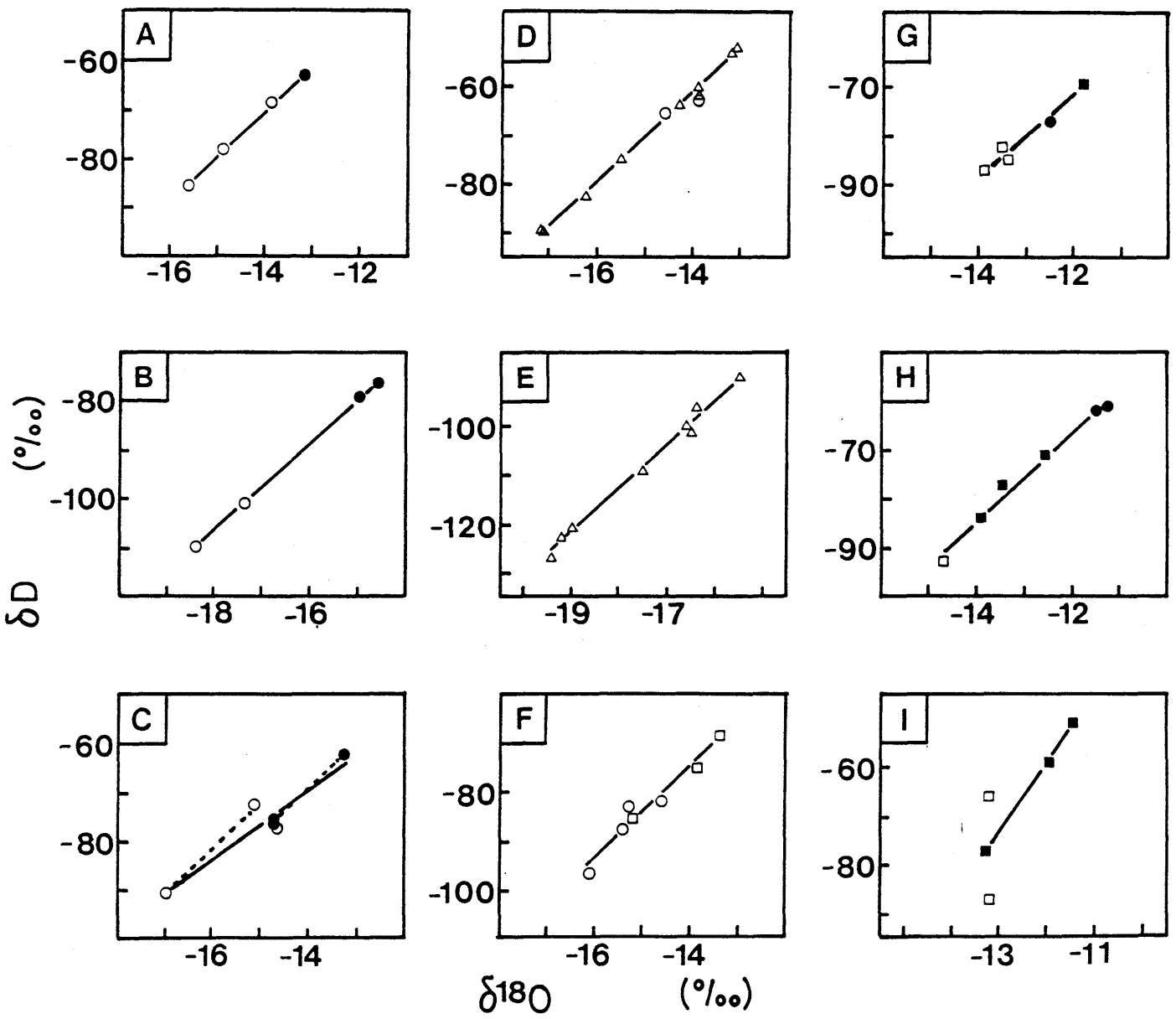

Fig. 4-1 Relationship between δD and $\delta^{18}O$ values of falling snow particles collected at windward station (closed circles and triangles) and leeward station (open circles, triangles and squares) for cases A - I. Type of snow particles was

circles:graupel

triangles: non-rimed snowflake

squares: rimed snowflake.

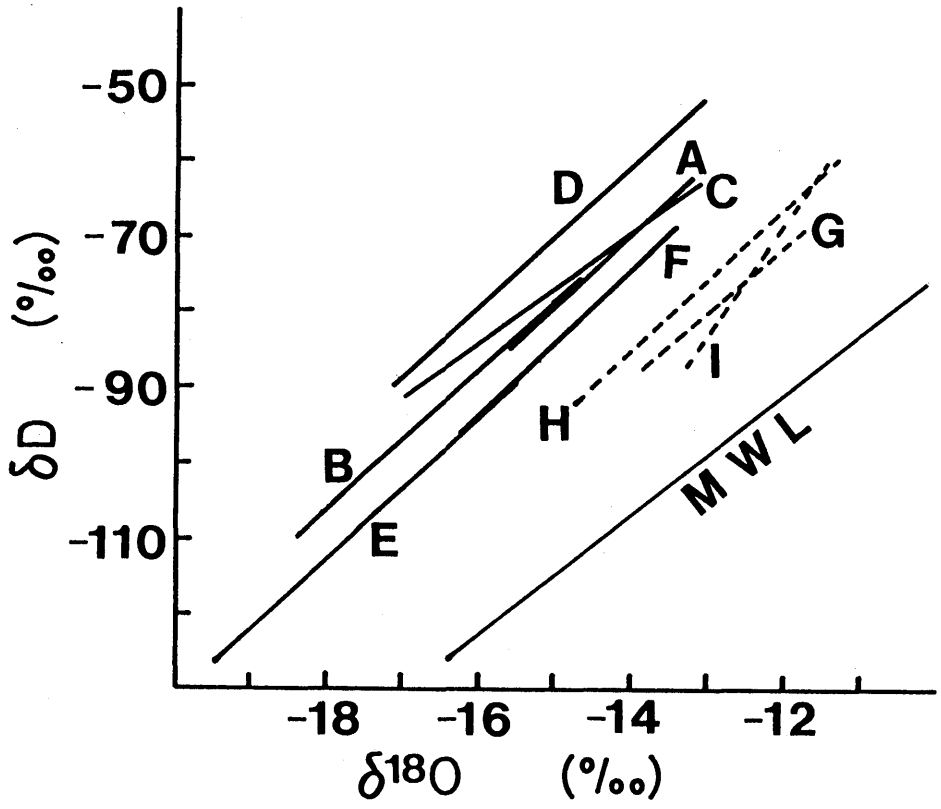

Fig. 4-2 Regression lines for cases A - I. Lines for cases A - F were obtained in Ishikari plain (solid line) and that for cases G - I in Hokuriku (broken line). The meteoric water line (MWL) is shown for comparison.

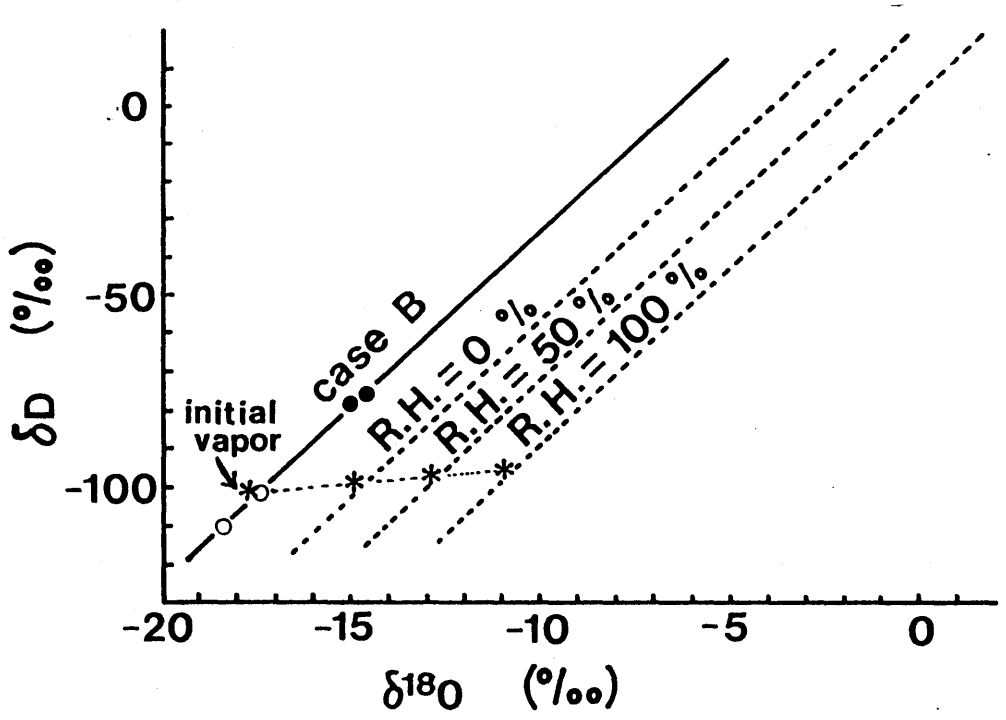

Fig. 4-3 Relationship between δD and $\delta^{18}O$ values of cloud droplets calculated for various isotopic compositions of initial vapor (asterisks) with temperature from -11°C to -29°C and initial pressure of 950 hPa.

Broken lines: the isotopic compositions of initial vapor are calculated from the model by Merlivat and Jouzel (1979) for relative humidities R.H.= 0, 50 and 100 %, assuming that friction velocity u_* = 40 cm/sec at the height of 10 m and sea surface temperature is 5°C.

Solid line: the isotopic composition of initial vapor is chosen so that the data points (open and closed circles) obtained from case B exist on this line, extending beyond the δD and $\delta^{18}O$ values of initial vapor for R.H.=0 %.

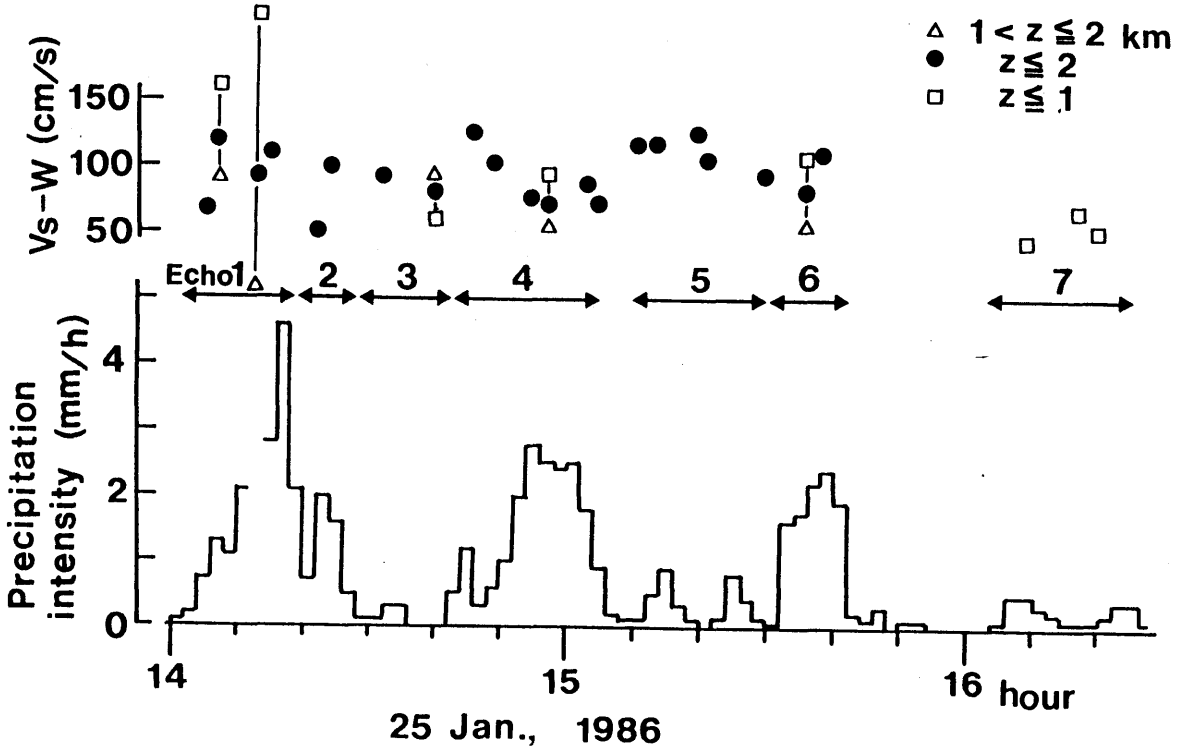

Fig. 5-1 Precipitation intensity and average falling velocity of snow particles observed by Doppler radar at the leeward station. In case in which the difference of falling velocity between upper and lower parts of the cloud is more than 40 cm/s, values for both upper and lower parts are shown.

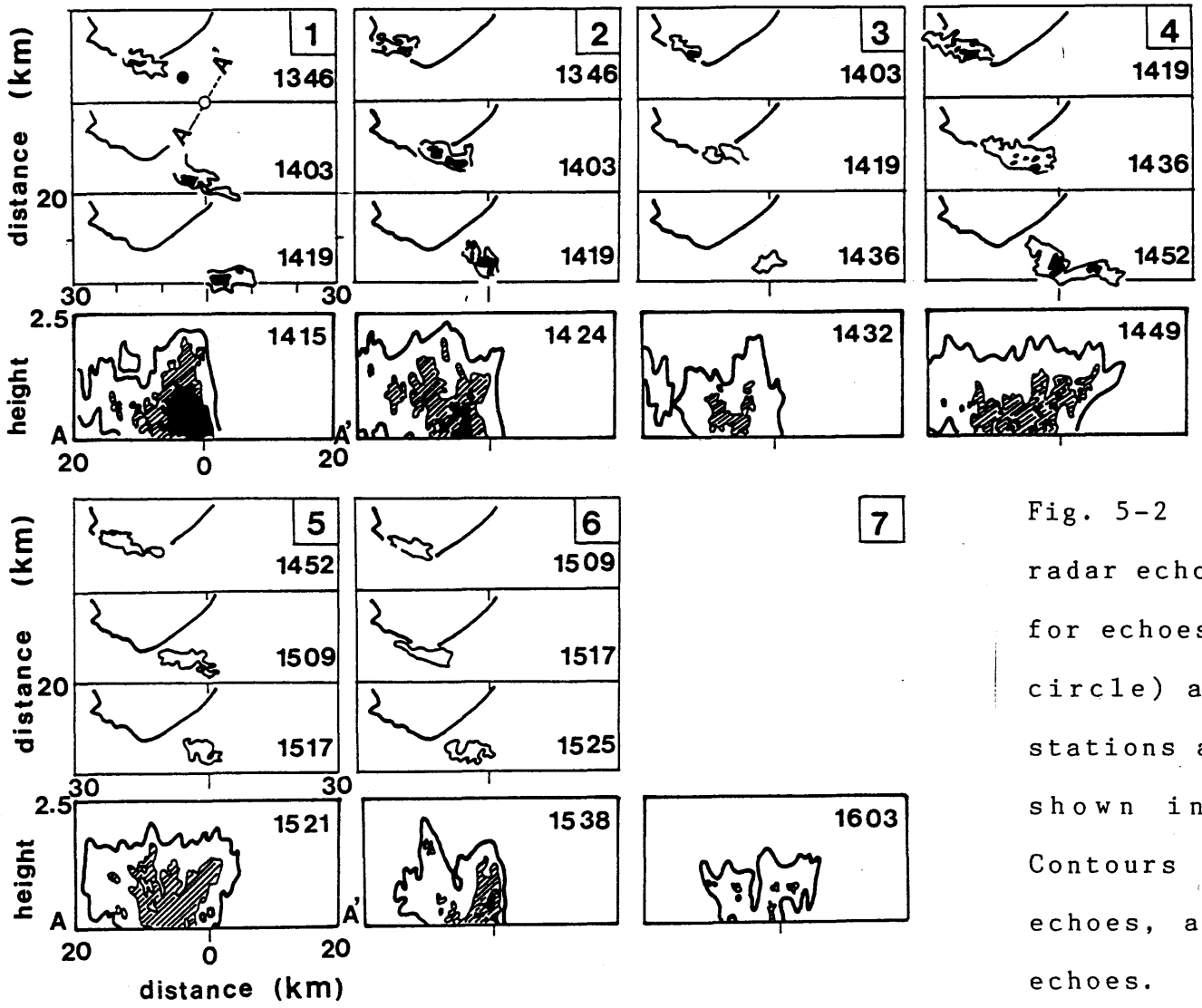

Fig. 5-2 PPI radar echoes and RHI radar echoes of A-A' cross section, for echoes 1 to 7. Windward (closed circle) and leeward (open circle) stations and the direction of A-A' are shown in the figure for echo 1. Contours are 19 and 24 dBZ in PPI echoes, and 10, 19 and 24 dBZ in RHI echoes. In echo 7, echo intensity is less than 19 dBZ.

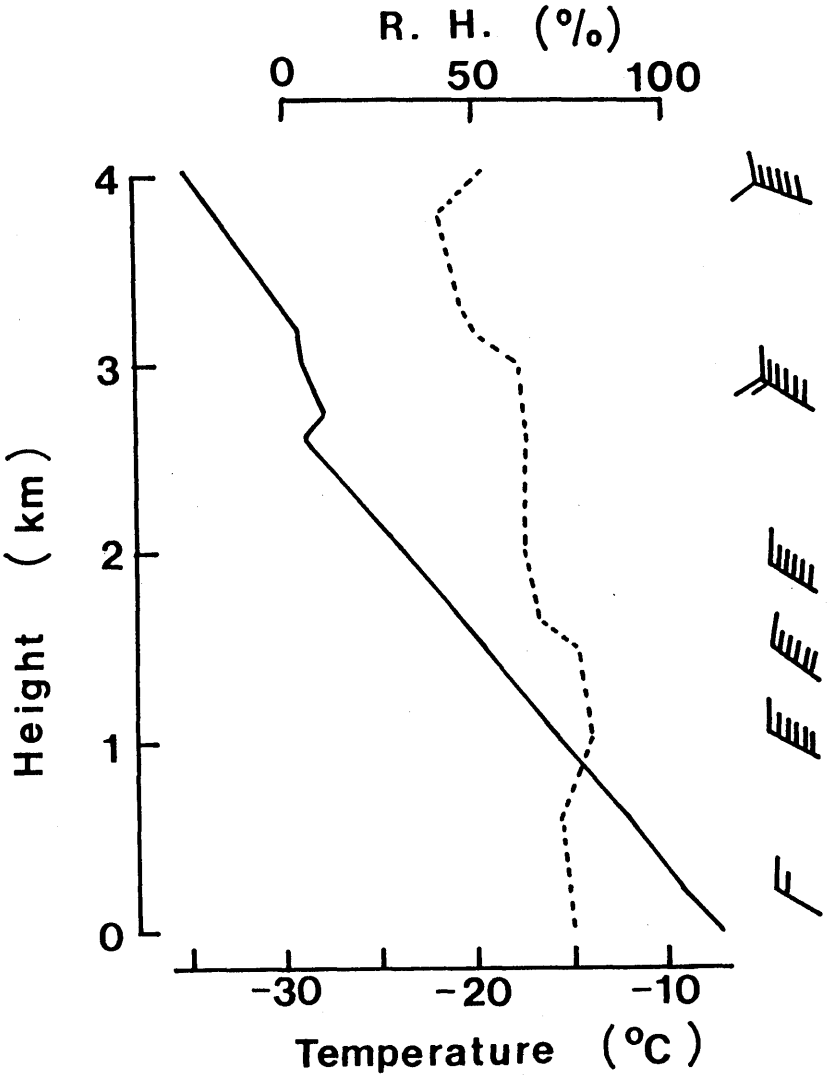

Fig. 5-3 Radiosonde data of air temperature (solid line), relative humidity (broken line) and wind direction and speed, at Sapporo at 09:00 (J.S.T.) on Jan. 25, 1986.

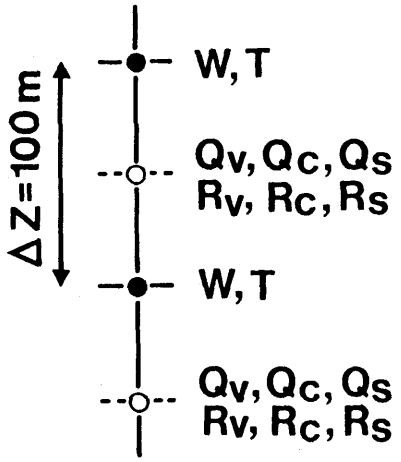

Fig. 6-1 Distribution of vertical grid points.

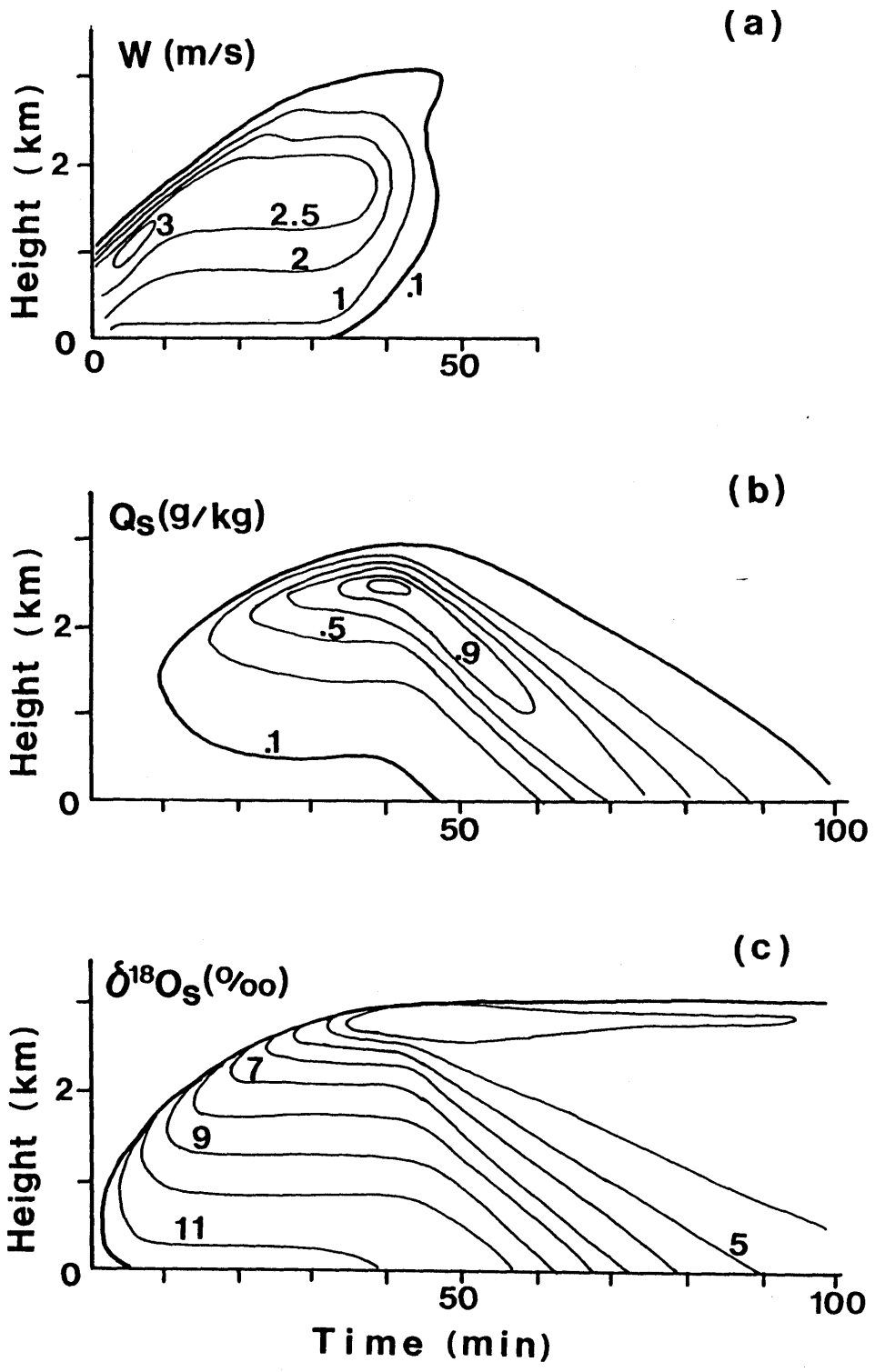

Fig. 6-2 Time-height cross section of vertical velocity of air W (a), mixing ratio of solid Q_s (b), $\delta^{18}O$ values of solid $\delta^{18}O_s$ (c), variations of vertical profiles of $\delta^{18}O$ of vapor $\delta^{18}O_v$ (d) and solid $\delta^{18}O_s$ (e) and variations of $\delta^{18}O_s$ and precipitation intensity at the surface (f) for case R1.

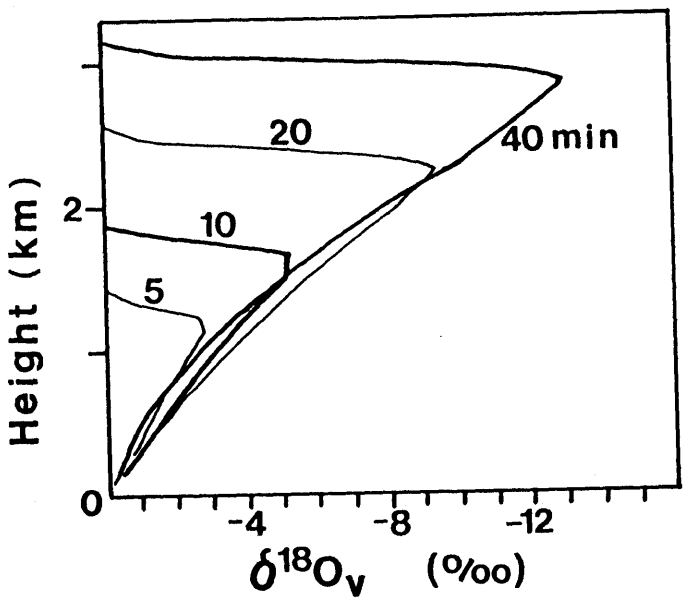
(d)
Height (km)
2
0
20
40 min
10
5
-4
-8
-12
δ18Ov (‰)

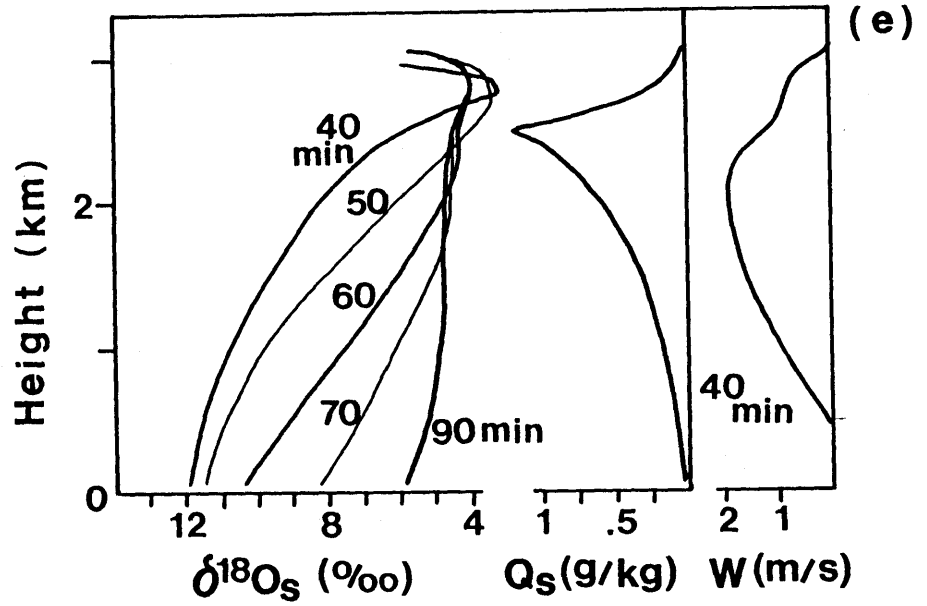
(e)
Height (km)
2
0
40 min
50
60
70
90 min
40 min
12
8
4
1
.5
2
1
δ18Os (‰)
Qs(g/kg)
W(m/s)

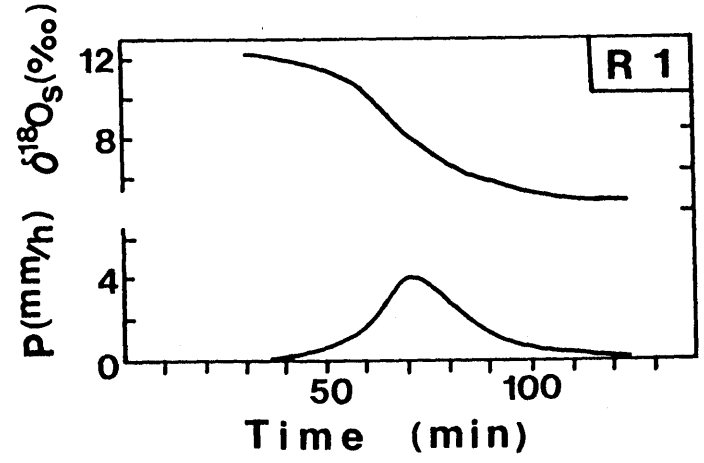
(f)
R 1
δ18Os(‰)
12
8
P(mm/h)
4
0
50
100
Time (min)

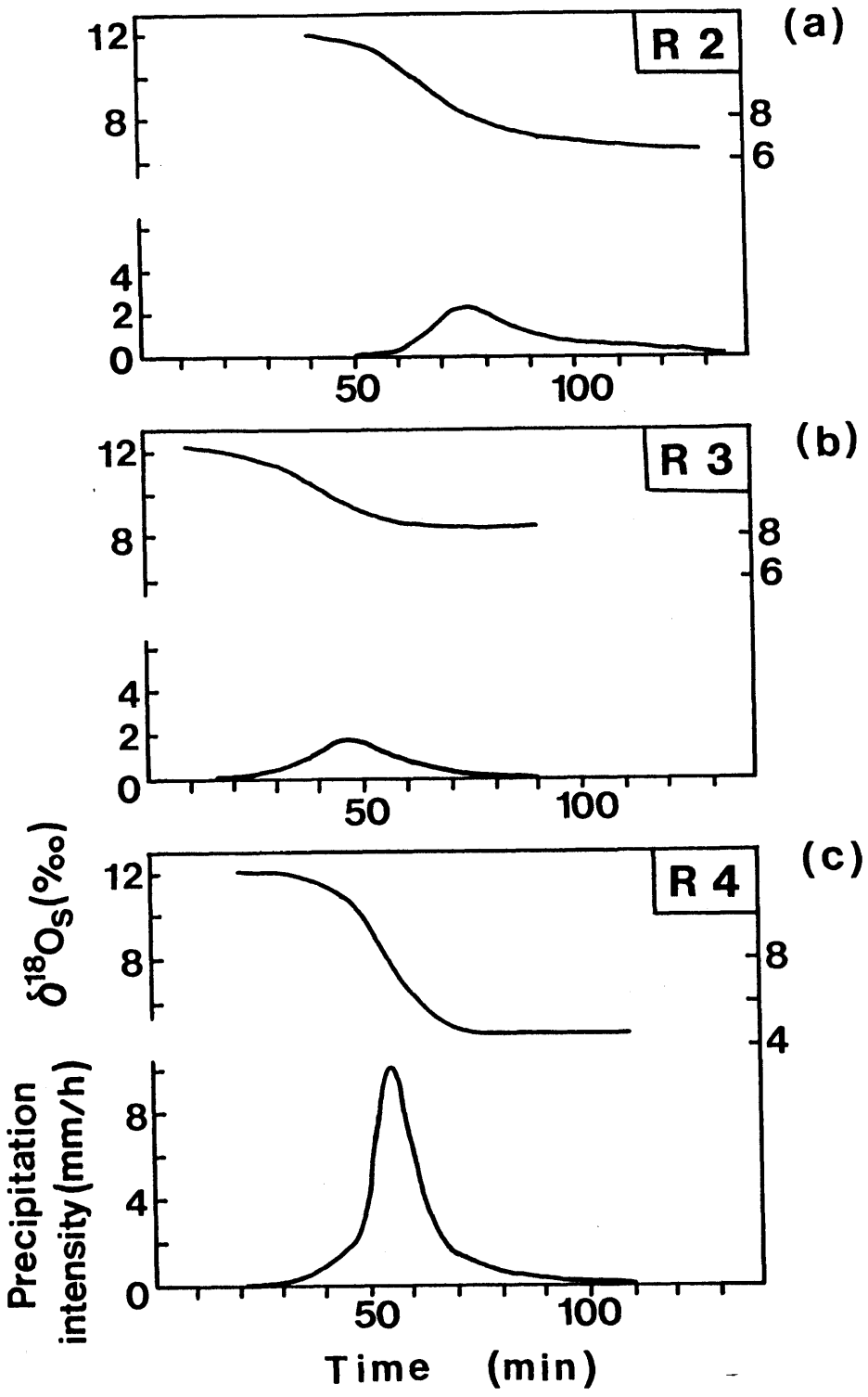

Fig. 6-3 Variations of $\delta^{18}O$ values of solid $\delta^{18}O_s$ and precipitation intensity at the surface for cases R2 (a), R3 (b) and R4 (c).

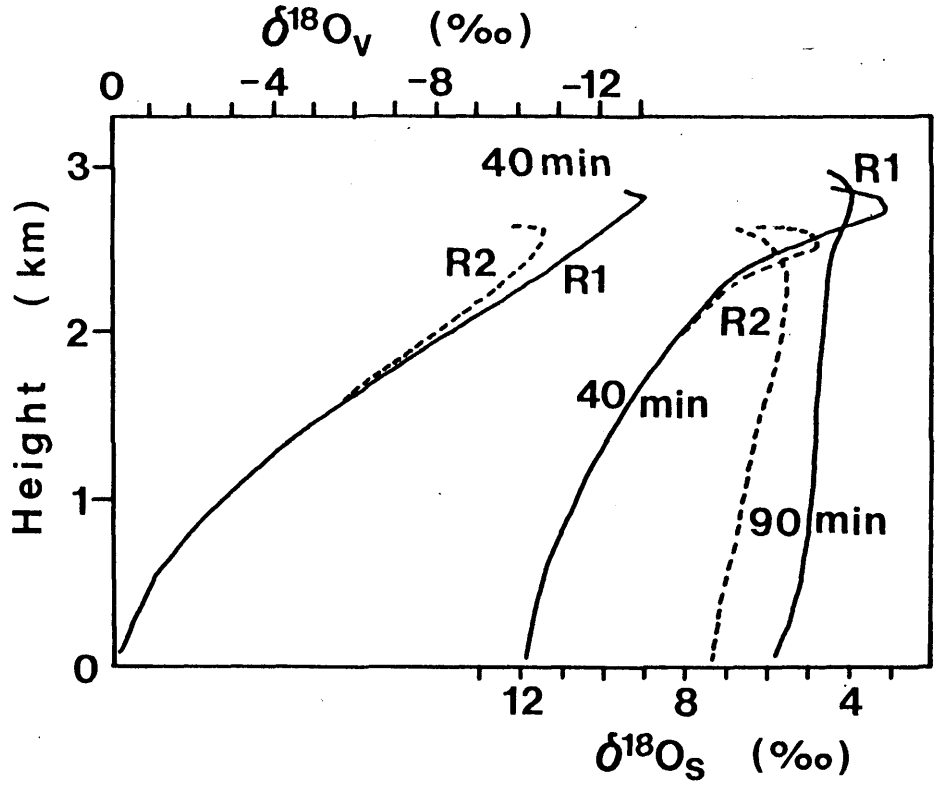

Fig. 6-4 Comparison of vertical profiles of $\delta^{18}O$ of vapor $\delta^{18}O_v$ and solid $\delta^{18}O_s$ between R1 and R2.

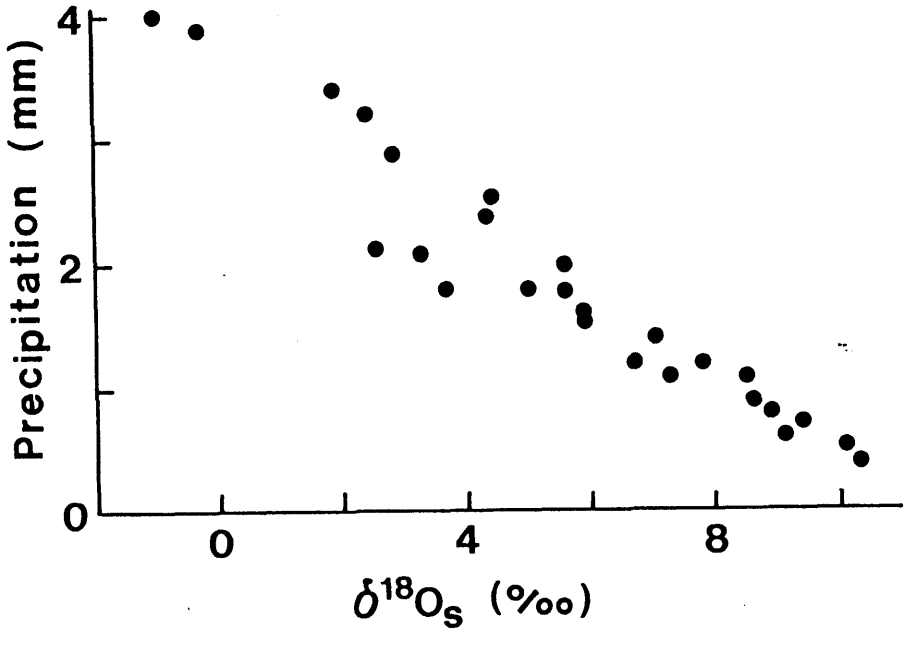

Fig. 6-5 Total amount of precipitation and $\delta^{18}O_s$ in the last stage of the cell.

Acknowledgement

I would like to thank Prof. G. Wakahama, Dr. Y. Fujiyoshi, Institute of Low Temperature Sience, Hokkaido University and collaborators for providing me with radar observation data, and Mr. Y. Aoki for help with observation. I would like to also thank Prof. M. Kusakabe for the guidance of deuterium mesuring. I am grateful to Prof. O. Matsubaya, Akita University, for valuable discussions and for encouragement.

Reference

Asai, T. and Kasahara, A. 1967: A theoretical study of the compensating downward motions associated with cumulus clouds. J. Atmos. Sci. 24, 487-496.

Aldaz, L. and Deutsch, S. 1967: On a relation between air temperature and oxygen isotope ratio of snow and firn in the south pole region. Earth Planet. Sci. Letters 3, 267-274.

Brutseart, W. 1975a: A theory for local evaporation (or heat trasfer) from rough and smooth surface at ground level. Water Resour. Res. 11, 543-550.

Brutseart, W. 1975b: The roughness length for water vapor, sensible heat, and other scalars. J. Atmos. Sci. 32, 2028-2031.

Craig, H. 1961: Isotopic variations in meteoric waters. Sience 133, 1702-1703.

Craig, H. and Gordon, L. H. 1965: Isotopic oceanography: Deuterium and oxygen-18 variations in the ocean and marine atmosphere. Marine geochemistry, Proc. Symp. at the Univ. Rhode Island, 1964, 277-374

Dansgaard, W. 1964: Stable isotopes in precipitation. Tellus 16, 436-468.

Epstein, S., Sharp, R. P. and Goddard, I. 1963: Oxygen-isotope ratios in Antarctic snow, firn and ice. J. Geol. 71, 698-720.

Federer, B., Brichet, N. and Jouzel. J. 1982a: Stable isotopes in hailstone. Part I: The isotopic cloud model. J. Atmos. Sci. 39, 1323-1335.

Federer, B., Thalmann, B. and Jouzel, J. 1982b: Stable isotopes in hailstones. Part II: Embryo and hailstone growth in

different storms. J. Atmos. Sci. 39, 1336-1355.

Friedman, I., Machta, L. and Soller, R. 1962: Water-vapor excahnge between a water droplet and its environment. J. Geophys. Res. 67, 2761-2766

Fujiyoshi, Y., Wakahama, G. and Kato, K. 1986: Short-term variation of oxygen isotopic composition of falling snow particles. Tellus 38B, 353-363.

Gedzelman, S. D. and Lawrence, J. R. 1982: The isotopic composition of cyclonic precipitation. J. App. Meteorol. 21, 1385-1404.

Higuchi, K. 1963: The band structure of snowfalls. J. Meteorol. Soc. Japan 41, 53-70.

Higuchi, K. 1982: Dependence of oxygen isotopic composition of surface snow on distance from coast in Mizuho plateau. Mem. Natl. Inst. Polar Res., Spec. Issue 24, 122-126.

Higuchi, K., Tokuoka, A. and Watanabe, O. 1985: Effects of precipitation on the isotopic composition of falling snow particles. Ann. Glaciol. 6, 261-262.

Itagaki, K. 1967: Self-diffusion in single crystal ice. J. Phys. Soc. Japan. 22, 427-431.

Jouzel, J., Merlivat, L. and Roth, E. 1975: Isotopic study of hail. J. Geophys. Res. 80, 5015-5030.

Jouzel, J. and Souchez, R. A. 1982: Melting-refreezing at the glacier sole and the isotopic composition of the ice. J. Glaciol. 28, 35-42.

Jouzel, J. and Merlivat, L. 1984: Deuterium and Oxygen 18 in precipitation: Modeling of the isotopic effects during snow formation. J. Geophys. Res. 89, 11749-11757.

Jouzel, J., Merlivat, L. and Federer, B. 1985: Isotopic study of

hail: The δD-$\delta^{18}O$ relationship and the growth history of large hailstones. Quart. J. Roy. Meteorol. Soc. 111, 495-516.

Jouzel, J., Russell, G. L., Suozzo, R. J., Koster, R. D., White, J. W. C. and Broecker, W. S. 1987: Simulations of the HDO and $H_2{}^{18}O$ atmospheric cycles using the NASA GISS general circulation model: The seasonal cycle for present-day conditions. J. Geophys. Res. 92, 14739-14760.

Kato, K. 1978: Factors controlling oxygen isotopic composition of fallen snow in Antarctica. Nature 272, 46-48.

Kusakabe, M., Wada, H. and Matsuo, S. 1970: Oxygen and hydrogen isotope ratios of monthly collected waters from Nasudake volcanic area, Japan. J. Geophys. Res. 75, 5941-5951.

Lawrence, J. R., Gedzelman, S. D., White, J. W. C., Smiley, D. and Lazov, P. 1982: Storm trajectories in eastern US D/H isotopic composition of precipitation. Nature 296, 638-640.

Macklin, W. C., Merlivat, L. and Stevenson, C. M. 1970: The analysis of a hailstone. Q. J. Roy. Meteorol. Soc. 96, 472-486.

Magono, C. 1965: The snow fall in the winter monsoon season of Japan. Proceedings of the International Conference on Cloud Phys. 1965 Tokyo and Sapporo, 502-511.

Majoube, M. 1970: Fractionation factor of ^{18}O between water vapour and ice. Nature 299, 1242.

Majoube, M. 1971: Fractionnement en oxygene 18 et en deuterium entre l'eau et sa vapeur. J. Chim. Phys. 10, 1423-1436. (in French)

Matsubaya, O. and Sakai, H. 1976: 地表水の水素および酸素同位体の挙動. 日本地球化学会年会講演要旨集, 121-122. (in Japanese)

Matsubaya, O. and Etchu, H. 1987: Hydrogen and oxygen isotope ratios of river water in the drainage system of Omono River. 秋田大学鉱山学部資源地学研究施設報告 52, 15-23 (in Japanese)

Merlivat, L. and Nief, G. 1967: Fractionnement isotopique lors des changements d'etat solide-vapeur et liquide-vapeur de l'eau a des temperatures inferieures a 0 C. Tellus 19, 122-127. (in French)

Merlivat, L. and Jouzel, J. 1979: Global climatic interpretation of the deuterium-oxygen 18 relationship for precipitation. J. Geophys. Res. 84, 5029-5033.

Miyake, Y., Matsubaya, O. and Nishihara, C. 1968: An isotopic study on meteoric precipitation. Pap. Meteorol. Geopys. 19, 243-266

Niewodniczanski, J., Grabczak, J., Baranski, L. and Rzepka, J. 1981: The altitude effect on the isotopic composition of snow in high mountains. J. Geol. 27, 99-111

Ogura, Y. and Takahashi, T. 1971: Numerical simulation of the life cycle of a thunderstorm cell. Mon. Wea. Rev. 99, 895-911.

Picciotto, E. and De Maere, X. 1960: Isotopic composition and temperature of formation of Antarctic snows. Nature 187, 857-859.

Rindsberger, M., Magaritz, M, Carmi, I. and Gilad, D. 1983: The relation between air mass trajectories and the water isotope composition of rain in the Mediterranean Sea area. Geophys. Res. Letters 10, 43-46.

Ronzanski, K. and Sonntag, C. 1982: Vertical distribution of deuterium in atmospheric water vapor. Tellus 34, 135-141.

Rozansi, K. Sonntag, C. and Munnich, K. O. 1982: Factors

controlling stable isotope composition of European precipitation. Tellus 34, 142-150.

Salati, E., Dall'Olio, A., Matsui, E. and Gat, J. R. 1979: Recycling of water in the Amazon basin: an isotopic study. Water Resour. Res. 15, 1250-1258

Satake, H., Oda, M., Mizutani, Y. and Kusakabe, M. 1982: Isotopic hydrology of precipitation and river water in the Toyama region, Japan. Proceedings of the Fifth International Conference on Geochronology Cosmochronology Isotope Geology, 336-337.

Sugimoto, A., Higuchi, K. and Kusakabe, M. 1988: Relation between δD and $\delta^{18}O$ values of falling snow particles from a separate cloud. Tellus 40B, 205-213.

Sugimoto, A. and Higuchi, K. 1989: Oxygen isotopic variation of falling snow particles with time during the lifetime of a clonvective cloud: Observation and modeling. Tellus (accepted)

Tsunogai, S., Fukuda, K. and Nakaya, S. 1975: A chemical study of snow formation in the winter-monsoon season: The contribution of aerosols and water vapor from the continent. J. Met. Soc. Japan 53, 203-212

Waseda, A. and Nakai, N. 1983: Isotopic composition fo meteoric and surface waters in central and northeast Japan. Chikyukagaku 17, 83-91 (in Japanese with English abstract)

Watanabe, O., Kanamori, N., Sugimoto, A., Iida, H. and Higuchi, K. 1986: Regional characteristics of snow cover in the mountain region of central Japan. J. Earth Sci. Nagoya Univ. 34, 67 to 108.

Woodcock, A. H. and Friedman I. 1963: The deuterium content of raindrops. J. Geophys. Res. 68, 4477-4483

Yapp, C. J. 1982: A model for the relationships between precipitation D/H ratios and precipitation intensity. J. Geophys. Res. 87, 9614-9620.